William Lautert-Dutra

Impact of CDK12 mutation on immune response in prostate cancer

Faculdade de Medicina de Ribeirão Preto, Departamento de Genética, Ribeirão Preto, São Paulo, Brasil

2023

William Lautert-Dutra

Impact of CDK12 mutation on immune response in prostate cancer

Dissertação de mestrado apresentada ao Programa de Pós-Graduação em Genética da Faculdade de Medicina de Ribeirão Preto (FMRP-USP), como parte dos pré-requisitos para obtenção do título de Mestre em Genética. Área de concentração: Genética.

Universidade de São Paulo – USP

Faculdade de Medicina de Ribeirão Preto

Programa de Pós-Graduação em Genética

Supervisor: Prof. Dr Jeremy Andrew Squire

Faculdade de Medicina de Ribeirão Preto, Departamento de Genética,
Ribeirão Preto, São Paulo, Brasil

2023

William Lautert-Dutra
Impact of CDK12 mutation on immune response
in prostate cancer / William Lautert-Dutra. – Faculdade de Medicina de Ribeirão Preto, Departamento de Genética, Ribeirão Preto, São Paulo, Brasil, 2023-
79p. : il. (algumas color.) ; 30 cm.

Supervisor: Prof. Dr Jeremy Andrew Squire

Tese (Mestrado) – Universidade de São Paulo – USP
Faculdade de Medicina de Ribeirão Preto
Programa de Pós-Graduação em Genética, 2023.

1. Biomarcadores. 2. Câncer de próstata. 3. Imunoterapia. 4. Transcritoma. 5. Bioinformática. I. Universidade de São Paulo. II. Faculdade de Medicina de Ribeirão Preto, Departamento de Genética. III. Mestrado

William Lautert-Dutra

Impact of CDK12 mutation on immune response in prostate cancer

Dissertação de mestrado apresentada ao Programa de Pós-Graduação em Genética da Faculdade de Medicina de Ribeirão Preto (FMRP-USP), como parte dos pré-requisitos para obtenção do título de Mestre em Genética. Área de concentração: Genética.

Parecer _____. Faculdade de Medicina de Ribeirão Preto, Departamento de Genética, Ribeirão Preto, São Paulo, Brasil, de de 2023:

Prof. Dr Jeremy Andrew Squire
Orientador

Professor
Convidado 1

Professor
Convidado 2

Faculdade de Medicina de Ribeirão Preto, Departamento de Genética,
Ribeirão Preto, São Paulo, Brasil

2023

Dedico à minha mãe
e a todos meus familiares e amigos que me ajudaram chegar até aqui.

Acknowledgements

Primeiramente, gostaria de agradecer ao meu orientador, **Prof. Dr. Jeremy Andrew Squire**, por sua generosidade e atenção durante sua orientação. Agradeço por confiar em mim o desenvolvimento desse projeto e por acreditar nas minhas ideias iniciais na elaboração deste trabalho. Agradeço pela sua paciência e prontidão em me atender em qualquer momento, por sua vontade em ajudar e estimular minha carreira. Agradeço também pela oportunidade de participar e de desenvolver colaborações que surgiram ao longo desses dois anos. Agradeço pela instrução e atenção durante os momentos de discussão sobre a melhor forma de escrever e editar o meus textos e, acima de tudo, por me guiar a manter o rigor do método científico.

Agradeço aos meus colegas do meu grupo de pesquisa, **André Luiz Caliari**, **Drª Camila Morais Melo**, **Francisco César** e **Luiz Paulo Chaves**, por todo o apoio e compreensão durante esses dois anos. Agradeço especialmente a Camila Melo por ser um dos elos mais importantes do nosso trabalho e por sua dedicação e generosidade para o nosso grupo. Obrigado, colegas.

Agradeço a minha família, em especial a minha mãe, **Elisângela da Costa Lautert**, que me apoiou incondicionalmente mesmo durante as maiores dificuldades. Agradeço seu carinho e incentivo durante todo meu caminho até aqui. Agradeço por não duvidar do meu potencial e por acreditar nas minhas capacidades. Agradeço também a minha tia **Maria Lautert** e tio **Miguel Pires** por abrirem as portas de sua casa durante minha graduação e possibilitarem que eu seguisse em frente. Agradeço à minha irmã **Cindy Lautert Dutra** por seu carinho e pela companhia. Agradeço meu primo e amigo **Fábio Fruhauf** por sua parceria e por sempre ter um tempo para conversar e me atender quando eu precisei. Estendo meu agradecimento aos meus outros familiares, os quais sempre foram parte essencial da minha vida. Agradeço pelo amor de vocês.

Agradeço à minha namorada **Antonia Angeli Gazola** por sua companhia e carinho. Agradeço por seu amor e paciência em momentos difíceis e decisivos nesses últimos anos. Agradeço também os meus sogros, **Fúlvia Angeli Gazola** e **José Rodrigo Gazola**, por estarem juntos nessa história e por confiarem em mim. Agradeço pelo amor de vocês.

Agradeço aos meus amigos, **Patrick D. de Souza** e **Daniel Tirapeli** por dividirem seu espaço comigo em Ribeirão Preto e pelos bons momentos juntos. Agradeço também meus amigos **Artur**, **Edgar**, **Eduarda**, **Dmitri**, **Levi**, **Luiza**, **Iago**, **Juliano**, **Oriel**, **Valdez** e **Yan**, pelas conversas, pelos momentos compartilhados, pela companhia e pelo seu tempo.

Agradeço a todos os professores que fizeram parte da minha formação. Agradeço os professores **João Roberto Fernandes** e **Susie**, **Prof. Vilmar Bittencourt**, por confiarem na minha capacidade. Agradeço o **Prof. Dr. Carlos Alberto de Lucena**, meu primeiro orientador de iniciação científica, o qual sempre me incentivou e que se tornou um grande amigo. Agradeço o **Prof. Maurício Bogo**, que me orientou durante minha graduação, por seu carinho e compreensão e que também se tornou um grande amigo. Agradeço o **Prof. Dr. Sandro Bonatto**, que me recebeu de braços abertos na fase final do meu projeto. Agradeço também à **Dra. Talita Pereira** e à **Dra. Giovanna Oliveira**, pela sua colaboração e amizade.

Agradeço o Departamento de Genética da Faculdade de Medicina de Ribeirão Preto, em especial à Secretária **Susie Nalon** e o **Prof. Dr. Klaus Hartmann Hartfelder**, pela assistência necessária para o desenvolvimento desse projeto. Agradeço ao **Luiz Antonio Framartino Bezerra** e ao **Sebastiao Paulo Framartino Bezerra** pela ajuda técnica no início desse projeto. Agradeço também aos outros funcionários da universidade. Agradeço a **Universidade de São Paulo** pela estrutura e oportunidade de desenvolver meu projeto. Agradeço à **Pontifícia Universidade Católica do Rio Grande do Sul**, pela estrutura e por me receber durante parte do projeto.

Agradeço a Coordenação de Aperfeiçoamento de Pessoal de Nível Superior **(CAPES)**, a Fundação de Apoio ao Ensino, Pesquisa e Assistência do Hospital das Clínicas de Ribeirão Preto **(FAEPA)** e o Conselho Nacional de Desenvolvimento Científico e Tecnológico **(CNPq)**, Coordenação de Aperfeiçoamento de Pessoal de Nível Superior – Brasil **(CAPES)**, e a Fundação de Amparo à Pesquisa do Estado de São Paulo **(FAPESP)** pelo financiamento deste projeto.

O presente trabalho foi realizado com apoio da Coordenação de Aperfeiçoamento de Pessoal de Nível Superior – Brasil (CAPES) – Código de Financiamento 001 e pela Fundação de Amparo à Pesquisa do Estado de São Paulo (FAPESP) - número do processo 2021/12271-5.

Resumo

Impacto da mutação de *CDK12* na resposta imune do câncer de próstata.

A inativação da quinase dependente de ciclina 12, *CDK12*, tem sido usada como um biomarcador preditivo da resposta ao tratamento ao bloqueio de checkpoint imunológico (Immune-checkpoint blokade, ICB) no câncer de próstata avançado (Prostate Cancer, PCa). No entanto, alguns pacientes com alterações de *CDK12* não respondem ao ICB. As alterações na expressão do MHC têm sido associadas à progressão do tumor e à redução da resposta ao ICB em diferentes malignidades. Usando dados públicos de transcriptoma e exoma de pacientes com *CDK12* mutado em tumores prostáticos primário (n=48) e metastático (n=10), investigamos a variação na expressão dos genes do MHC e as alterações moleculares associadas. Dividimos os tumores em níveis de expressão "Alto" e "Baixo" de MHC-I e -II com base nos quartis de expressão gênica. Tumores defeituosos de *CDK12* com níveis aumentados de MHC mostraram a ativação de várias vias associadas ao sistema imunológico e expressão elevada de *PD-L1, IDO1* e *TIM3*. Houve também aumento da composição de células T CD8+, células B, células T γδ e macrófagos M1 em tumores com mutação CDK12 com níveis elevados de MHC. Em contraste, tumores defeituosos de *CDK12* com expressão reduzida de MHC foram frequentemente sujeitos a eventos genômicos de perda de heterozigosidade (LOH) afetando MHC-I/-II e o agrupamento de genes HLA no cromossomo 6. Nossos dados sugerem que PCa com *CDK12* mutado expressa níveis mais altos do MHC clássico e têm um microambiente tumoral ativo e inflamado com expressão elevada da via imunomoduladora e presença aumentada de células T efetoras. O achado de menor expressão do MHC em tumores com LOH de genes associados no cromossomo 6 sugere que a expressão reduzida do MHC pode ser causada pela aquisição de eventos genômicos somáticos específicos que reduzem a expressão desses genes apresentadores de antígenos. Coletivamente, esses dados indicam que a implementação de uma medida combinada de mutação de *CDK12* e níveis de expressão de MHC, juntamente com uma avaliação do status de LOH, po de prever melhor os resultados de tumores de câncer de próstata classificados como elegíveis para tratamento com ICB.

Palavras-chave: Biomarcadores, Câncer de Próstata, Imunoterapia, Transcriptomica, Bioinformática

Abstract

The inactivation of Cyclin-dependent Kinase 12, *CDK12*, has been used as a predictive biomarker of treatment response to immune-checkpoint blockade (ICB) in advanced prostate cancer (PCa). However, some patients with *CDK12* alterations fail to respond to ICB. Changes in MHC expression have been linked to tumor progression and reduced response to ICB in different malignancies. Using public domain transcriptome and WES data from the primary (n=48) and metastatic (n=10) *CDK12* defective PCa, we investigated variation in the expression of the MHC genes and associated downstream changes. Based on gene expression quartiles, we divided the tumors into "High" and "Low" expression levels of MHC-I and -II. CDK12 defective tumors with increased MHC levels showed the activation of several pathways associated with the immune system and elevated *PD-L1, IDO1*, and *TIM3* expression. There was also an increased composition of CD8+ T cells, B cells, γδ T cells, and M1 Macrophages in *CDK12* mutated tumors with elevated MHC levels. In contrast, *CDK12* defective tumors with decreased MHC expression were often subject to loss of heterozygosity (LOH) genomic events affecting MHC-I/-II and the HLA gene cluster on chromosome 6. Our data suggest that *CDK12* defective PCa express higher levels of classical MHC and have an active and inflamed tumor microenvironment with elevated immunomodulatory pathway expression and increased presence of effector T cells. The finding of lower MHC expression in tumors with LOH of associated genes on chromosome 6 suggests reduced MHC expression may be caused by the acquisition of specific somatic genomic events that reduce the expression of these antigen presentation genes. Collectively, these data indicate that implementing a combined measure of *CDK12* mutation and MHC expression levels together with an evaluation of LOH status may better predict outcomes for prostate cancer tumors classified as eligible for ICB treatment.

Keywords: Biomarkers, Prostate Cancer, Immunotherapy, Transcriptomic, Bioinfomatics

List of Figures

List of Tables

List of abbreviations and acronyms

ADT	Androgen Deprivation therapy
APC	ABsurdas Normas para TeX
CDK12	Cyclin-dependent Kinase 12
CN-LOH	Copy-neutral loss of heterozygosity
dbGaP	The database of Genotypes and Phenotypes
DDR	DNA damage repair
DEGs	Differentially expressed genes
FACETS	Fraction and Allele-Specific Copy Number Estimated from Tumor Sequencing
FDR	False discovery rate
GEP	Gene expression profile
GO	Gene ontology
ICB	Immune-checkpoint blockade
LM22	Leukocyte gene signature matrix
LOH	loss of heterozygosity
mCRPC	Metastatic Castration-Resistant Prostate Cancer
MHC	Major histocompatibility complex
MSigDB	Molecular Signature Database
NCCN	National Comprehensive Cancer Network
ORA	Over-representation analyses
PCa	Prostate Cancer
PE	Paired-end
pPCa	Primary prostate cancer
PRAD	Prostate Adenocarcinoma

PSA Prostate-specific antigen

TCGA-PRAD The Cancer Genome Atlas

TME Tumor microenvironment

LOH Loss-of-Heterozygosity

Contents

Part I

Part I

Quantitative MHC class-I/-II gene expression levels in CDK12 mutated prostate cancer reveal intratumoral T cell adaptive immune response in tumors.

William Lautert-Dutra[1], Camila M. Melo[1],
Luiz P. Chaves[1], Rodolfo B. dos Reis[2],
Sandro L. Bonatto[3] and Jeremy A. Squire[1,4,*]

[1] Department of Genetics, Ribeirão Preto School of Medicine, University of São Paulo, Ribeirao Preto 14048-900, SP, Brazil.

[2] Division of Urology, Department of Surgery and Anatomy, Ribeirão Preto School of Medicine, University of São Paulo, Ribeirao Preto 14048-900, SP, Brazil.

[3] School of Health and Life Sciences, Pontifical Catholic University of Rio Grande do Sul, Av. Ipiranga, 668, 90619-900, Porto Alegre, RS, Brazil

[4] Department of Pathology and Molecular Medicine, Queen's University, Kingston, ON K7L3N6, Canada.

*Corresponding author: Department of Genetics, Ribeirao Preto School of Medicine, University of São Paulo, Ribeirao Preto 14048-900, SP, Brazil. Tel.: + 55 16 3602-3252; E-mail: squirej@fmrp.usp.br.

This research was funded by FAPESP, grant numbers 2019/22912-8 (JAS), 2021/12271-5 (WLD), and by CNPq grant PQ-1D to JAS.

1 Introduction

Treatment of advanced prostate cancer (PCa) remains a therapeutic challenge. Men with distant metastases at diagnosis have the worst overall survival (OS), with only 30 % of patients surviving > 5 years (1). For recurrent disease, acquired resistance to androgen deprivation therapy (ADT) and chemotherapy remains a significant cause of death (2). Immune-checkpoint blockade (ICB) therapies, such as PD-L1 inhibition, have shown only significant benefits in a minority of patients (3). Thus, it is necessary to discover and characterize the genetic pathways and molecular signatures that could help predict more effective disease progression control in advanced PCa.

The tumor mutation burden affects the infiltration of immune cells in the tumor microenvironment (TME) (4). Because of the high load of neoantigens, tumors with defective DNA damage repair (DDR) pathways are more suitable for immunotherapy (5). The biallelic inactivation of Cyclin-dependent Kinase 12, *CDK12*, was recently described as a novel immune active class of advanced PCa with a more aggressive phenotype, a high mutation burden derived from focal tandem duplication events, and high inflammatory and immune cell infiltrate distinct from other defective molecular subtypes (6, 7, 8, 9). Although this new subtype has been proposed as a predictive biomarker of treatment response to immune-checkpoint blockade (ICB) in advanced prostate cancer (PCa), many patients with *CDK12* alterations still fail to respond to ICB treatment. In a retrospective multi-center study, Antonarakis et al. found that just 33 % of the *CDK12*-altered advanced PCa patients had a prostate-specific antigen (PSA) response and an increased progression-free survival of 5.4 months when treated with anti-PD-1 therapy (10). In another study, Schweizer et al. showed that of the nineteen advanced patients who received ICB, eleven (59%) showed a response based on a decline in PSA, with two patients (11%) having a 100% PSA decline. However, the molecular causes of ICB resistance in this molecular subtype of PCa are poorly understood.

Tumor cells may develop various escape mechanisms that allow them to avoid recognition and destruction by the immune system. For example, the expression of checkpoint proteins (PD-1/PD-L1, CTLA-4, LAG3) by tumors can modulate the activity of immune infiltrate cells (11). Tumors may also develop intrinsic cancer-cell signaling that can suppress infiltrating immune cells (WNT/β-catenin) and increase pro-tumorigenic immune cell infiltration (Tregs, M2 Macrophages) in the TME (12, 13). Another mechanism exploited by tumors to avoid the recognition of cytotoxic T cells (CD8+) and antigen-presenting cells (APCs) is through loss of major histocompatibility complex class-I or class-II (MHC-I and MHC-II) (14).

Changes in MHC expression have been linked to tumor progression, poor prognosis, and reduced response to ICB in different malignancies (15, 16). As classified by Garrido et al., the alteration in the MHC expression can be divided into two major mechanistic groups: tumors with "Soft" alterations are capable of recovering or upregulating MHC antigens after cytokine exposure (e.g., they have regulatory abnormalities); those with "Hard" alterations cannot recover MHC expression (e.g., they have structural defects) (17). During tumor evolution, the infiltration of cytotoxic lymphocytes eliminates highly immunogenic tumor clones, causing a selection of surviving cell populations that have acquired MHC alterations through either "Soft" or "Hard" mechanistic alterations (18). Low expression of MHC-I and -II has been associated with poor prognosis and resistance to anti-CTLA-4 and anti-PD-1, respectively (19, 20). However, in PCa, there is presently limited information on the role of MHC-I and MHC-II expression and ICB response and if the low expression of antigen presentation mechanism could better predict the lack of response to ICB in *CDK12*-altered patients.

In prostate cancer, *CDK12* inactivation is known to increase the immunogenicity of tumor cells, but the relationship between *CDK12* loss and MHC expression has not been investigated. Changes in MHC-I and -II expression are involved in tumor immune evasion in various types of cancer. There is also evidence that higher expression of MHC genes can identify tumors likely to respond to ICB. However, the molecular and genomic mechanisms responsible for reducing MHC expression are poorly understood. Hence, we hypothesize that variation in the expression of the MHC genes could explain the lack of response to ICB in *CDK12* defective tumors. The findings suggest that *CDK12* defective PCa expressing higher MHC levels have an active and inflamed tumor microenvironment with elevated immunomodulatory pathway expression and increased presence of effector T cells. We also found that tumors with decreased MHC expression also showed loss-of-heterozygosity (LOH) of MHC-I/-II and the HLA gene cluster on chromosome 6 associated with MHC expression and antigen presentation. Collectively, these data suggest that implementing a combined measure between *CDK12* mutation and the presence of MHC expression may better predict outcomes for prostate cancer tumors classified as eligible for ICB treatment based on *CDK12* subtype and normal antigen presentation function.

2 Methods

We used The CbioPortal for Cancer Genomics (21) to search primary (pPCa) and metastatic castration-resistant (mCRPC) prostate tumors with *CDK12* mutated sample cohorts and to download matched clinical information. The classification of samples having **CDK12** loss-of-function followed previous reports (6, 7, 8, 9) based only on the presence of somatic mutations (non-synonymous mutations, deep deletions, and shallow deletions) in both *CDK12* alleles (*CDK12* defective). Only cohorts containing *CDK12* defective samples WES and with RNA-seq data were selected in the database of Genotypes and Phenotypes (dbGaP) database and applied for access under project ID 29255 (Figure 1, Table 1), Appendix B.

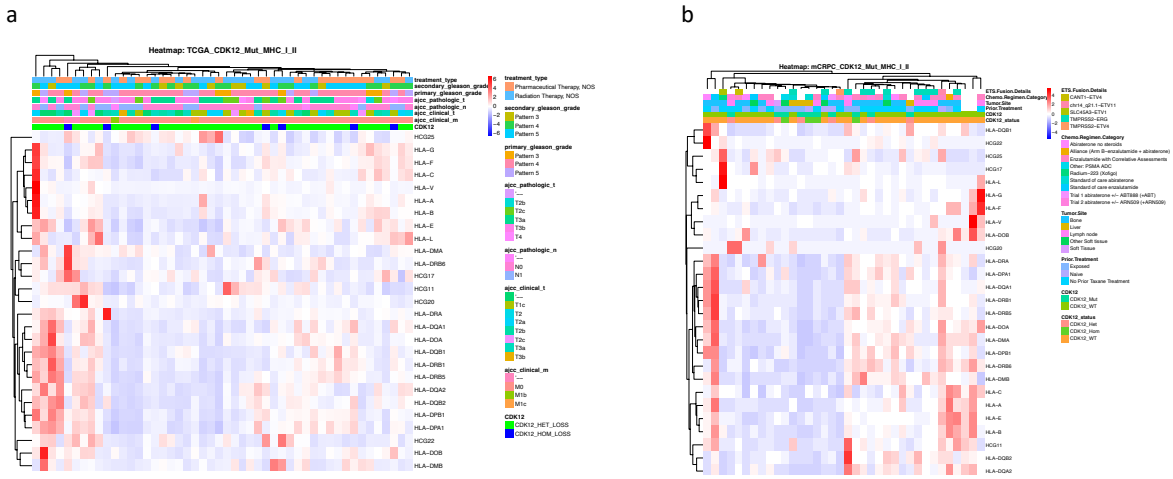

Figure 1 – HLA expression in *CDK12* patients.

Legend: We observed two groups of *CDK12* defective tumors regarding MHC expression using hierarchical clustering analysis for pPCa (a) and mCPRC (b). We then used the normalized expression level of each gene to classify the patients based on their MHC gene expression (See methods and Figure 2). The summary values used to classify the tumors are shown in Tables 1 2.

Count	Min.	1st Qu.	Median	Mean	3rd Qu.	Max.
HLA-A	216655	653123	1014248	1448456	1543897	13086664
HLA-B	624368	1937947	2854229	3369305	3991640	3991640
HLA-C	59691	178965	254295	300718	355755	1483674
HLA-DQA1	3606	33180	57044	75686	95324	286606
HLA-DQA2	3699	27917	68439	86416	131837	331294
HLA-DQB1	5590	34612	66553	104636	142415	407448
HLA-DQB2	2582	11144	26485	30166	43827	114119
HLA-DRA	212506	883473	1423990	1813254	1990959	12706556
HLA-DRB1	11460	66845	121649	149185	195939	654466
HLA-DRB5	32776	104569	186964	227375	286659	778600
HLA-DRB6	76.44	1019.97	2098.05	3174.20	4023.98	16588.38
HLA-DPA1	91078	399344	573795	665302	866957	1662374
HLA-DPB1	34050	150040	240450	285174	351060	992407

Table 1 – Summary information of the classical MHC genes TCGA PRAD.

Count	Min.	1st Qu.	Median	Mean	3rd Qu.	Max.
HLA-A	1674	6456	10584	11415	14377	23615
HLA-B	3710	10671	15404	16760	24770	30362
HLA-C	13084	17305	24154	26461	34955	45255
HLA-DQA1	141.8	837.6	2052.8	3037.4	4498.2	10065.9
HLA-DQA2	2.474	52.947	150.137	308.115	185.682	1921.254
HLA-DQB1	431.6	767.5	2133.5	2926.8	3528.0	10464.5
HLA-DQB2	12.35	40.49	219.94	263.24	402.19	799.87
HLA-DRA	809.1	7382.5	11255.5	14730.0	19322.9	38876.5
HLA-DRB1	314.3	2935.0	4975.7	6639.5	7342.5	18089.3
HLA-DRB5	64.08	587.09	2314.32	3967.07	4220.98	14692.93
HLA-DRB6	2.626	6.471	24.803	189.620	181.936	872.645
HLA-DPA1	436.5	1040.6	2472.7	3703.5	6269.0	8528.0
HLA-DPB1	943.1	2789.0	5445.6	7381.2	13247.5	14922.0

Table 2 – Summary information of the classical MHC genes mCRPC (SU2C).

Summary information of the classical MHC genes. We used an arbitrary cutoff of quartile to divide the *CDK12* defective tumors into "High" and "Low" expressed MHC-I and -II groups. For the quartile quantification, we used the normalized expression values of the classical genes that composed each MHC class (e.g., *MHC-I, HLA-A, HLA-B, HLA-C; MHC-II, HLA-DPA1, HLA-DPB1, HLA-DQA1, HLA-DQA1, HLA-DQB1, HLA-DQB2, HLA-DRA, HLA-DQB1, HLA-DRB5, HLA-DRB6*) (ref. 35). We dichotomized expression levels to be below or above the first quartile for each gene; we then used this classification to generate the final logical values regarding the patient's MHC status ('High' or 'Low' expressed)

2.1 Transcriptomic analysis

For the pPCa (TCGA-Prostate Adenocarcinoma, n = 48), we used the package recount2 to download summarized experiments objects containing the transcription-level RNA-Seq abundance matrix (22, 23). For the mCRPC (SU2C, n = 10), we downloaded SRA Paired-End (PE) reads using the SRAToolkit. The quality of the raw reads was then measured using the FASTQC program. We quantified the transcripts using the software Salmon v1.6.0 (24). The transcriptome index was built using the reference GRCh38 version of the human genome and transcriptome, downloaded from ENSEMBL and GENCODE, following the manual instruction. We then used the Tximport v1.22.0 package to import the transcription-level abundance and estimate raw counts derived from the quantification step. The count data normalization, expression levels, and differential gene expression (DEG) analysis for pPCa and mCRPC cohorts were executed using the DESeq2 v1.34.0 (25, 26). We used the clusterProfiler v4.2.1 to implement equally over-representation (ORA) enrichment analysis and gene set enrichment analysis (GSEA) of the DEGs and the whole transcriptome profile, respectively, using the Gene Ontology (GO) and Molecular Signatures Database (MSigDB) (27, 28, 29, 30, 31, 32)(Figure 1).

2.2 MHC expression

We performed a hierarchical clustering analysis using representative MHC genes. We observed two groups of *CDK12* defective tumors regarding MHC expression, as shown in 1. We dichotomized expression levels below or above the first quartile for each gene; we then used this classification to generate the final logical values regarding the patient's MHC status ('High' or 'Low' expressed) (Figure 2) (33, 34). For the quartile quantification, we used the normalized expression values of the classical genes that composed each MHC class (e.g., MHC-I: *HLA-A, HLA-B, HLA-C*; MHC-II: *HLA-DPA1, HLA-DPB1, HLA-DQA1, HLA-DQB1, HLA-DQB2, HLA-DRA, HLA-DRB5, HLA-DRB6*). Samples were classified as having MHC 'Low' expression when at least one gene composing each class was expressed at a low level. In mCRPC *CDK12*-defective, all tumors classified as MHC-High presented similar high expression of both MHC-I and -II; thus, we called these tumors just MHC High (henceforth, mCRPC *CDK12* defective MHC High). The summary values used to classify the tumors are shown in Tables 1 2.

2.3 Genomic Profile

We downloaded SRA Paired-End (PE) reads for both pPCa (n=48) and mCRPC (n=10) and processed them as previously described. The GRCh38 reference was sorted using the SeqKit (35). The final fastq files were then aligned to hg38 using bwa with

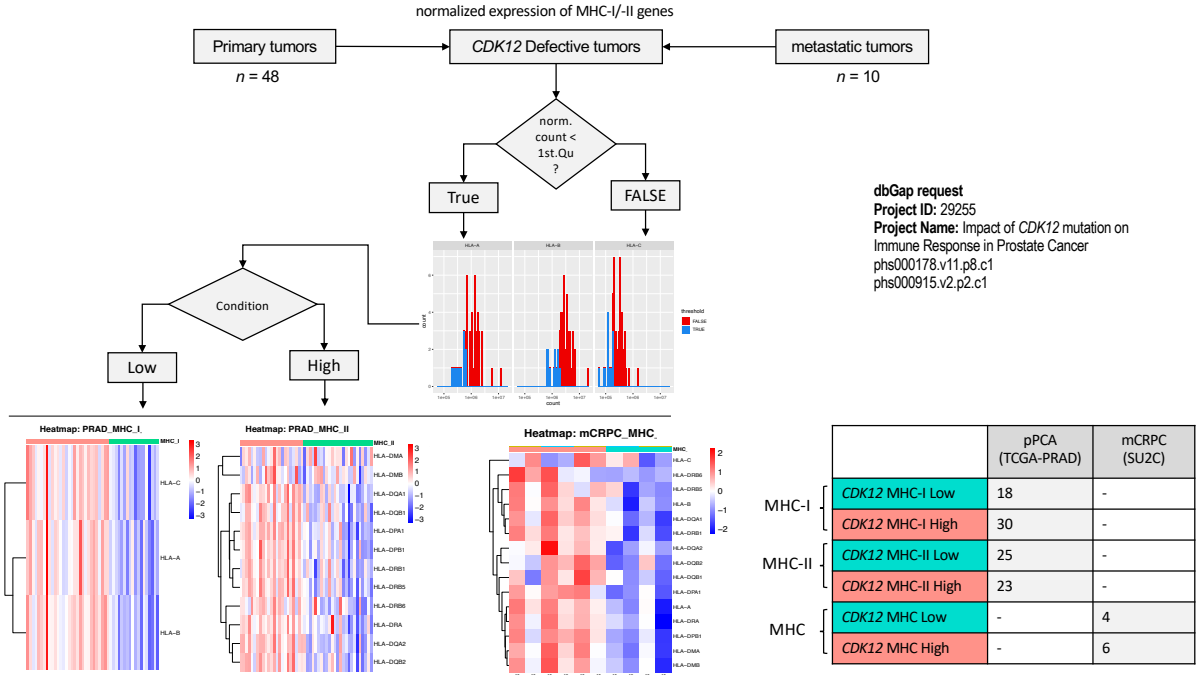

		pPCA (TCGA-PRAD)	mCRPC (SU2C)
MHC-I	*CDK12* MHC-I Low	18	-
	CDK12 MHC-I High	30	-
MHC-II	*CDK12* MHC-II Low	25	-
	CDK12 MHC-II High	23	-
MHC	*CDK12* MHC Low	-	4
	CDK12 MHC High	-	6

Figure 2 – Classification of *CDK12* patients based on HLA genes (MHC-I and -II) expression.

Classification of *CDK12* patients based on expression of HLA genes (MHC-I and -II). We used the normalized expression values of the classical genes that composed each MHC class (e.g., MHC-I: *HLA-A, HLA-B, HLA-C*; MHC-II: *HLA-DPA1, HLA-DPB1, HLA-DQA1, HLA-DQB1, HLA-DQB2, HLA-DRA, HLA-DRB5, HLA-DRB6*). We dichotomized expression levels below or above the first quartile for each gene using the normalized read count; we then used this classification to generate the final logical values regarding the patient's MHC status ('High' or 'Low' expressed) as follows: e.g., threshold *Gene 1* AND threshold *Gene 2* AND threshold *Gene 3*. Samples were classified as having MHC 'Low' expression when at least one gene composing each class was expressed at a low level. In mCRPC *CDK12*-defective, all tumors classified as MHC-High presented similar high expression of both MHC-I and -II; thus, we called these tumors just MHC High. The table above shows the final number of patients classified for each tumor type in each condition.

a penalty for up to 3 mismatches per read (36, 37). Sam files were converted to bam files and processed using samtools v1.16.1. To determine whether any MHC expression differences were related to genomic alterations, we used the FACETS (Fraction and Allele-Specific Copy Number Estimated from Tumor Sequencing) algorithm (38). We used this approach to assess matched normal-tumors WES and mutant allele-specific copy-number homozygous/heterozygous deletions, copy-number neutral loss-of-heterozygosity (LOH), allele-specific gain/amp in genomic loci associated with genes involved in antigen presentation (Table 3). Reference and variant allele read counts were extracted from the

bam file for common, polymorphic SNPs downloaded from dbSNP (GRCh38p7) using FACETS snp_pileup function with a minimum threshold for mapping quality, the minimum threshold for the base quality, and minimum read depth of 15, 20, 20, respectively. The pre-processing followed the suggested recommendations from the manual, and genomic intervals of 150-250bp were used to avoid hyper-segmentation in high polymorphic neighborhood regions. Mutant allele-specific copy-number changes were declared when the points changes were greater than a pre-determined critical value (cval) of 100 compared to constant copy-number regions.

Gene	chrom	start	end	bases	Cytogenetic band
JAK1	1	64,833,229	65,067,746	234,518	1p31.3
STAT1	2	190,968,989	191,014,197	45,209	2q32.2
IRF2	4	184,382,741	184,474,580	91,84	4q35.1
IRF1	5	132,481,609	132,490,773	9,165	5q31.1
HLA-A	6	29,942,532	29,945,870	3,339	6p22.1
HLA-B	6	31,353,875	31,357,179	3,305	6p21.33
HLA-C	6	31,268,749	31,272,092	3,344	6p21.33
HLA-DRA	6	32,439,887	32,445,046	5,16	6p21.32
HLA-DRB5	6	32,485,120	32,498,064	12,945	6p21.32
HLA-DRB6	6	32,520,490	32,527,799	7,31	6p21.32
HLA-DPA1	6	33,032,346	33,048,552	16,207	6p21.32
HLA-DPB1	6	33,043,703	33,054,978	11,276	6p21.32
HLA-DQA1	6	32,595,956	32,614,839	18,884	6p21.32
HLA-DQB1	6	32,627,244	32,636,160	8,917	6p21.32
HLA-DQB2	6	32,723,875	32,731,311	7,437	6p21.32
IFNGR1	6	137,197,484	137,219,385	21,902	6q23.3
TAP1	6	32,845,209	32,853,704	8,496	6p21.32
TAP2	6	32,821,831	32,838,739	16,909	6p21.32
JAK2	9	4,984,390	5,129,948	145,559	9p24.1
PTEN	10	87,863,625	87,971,930	108,306	10q23.31
B2M	15	44,711,492	44,718,145	6,654	15q21.1
CIITA	16	10,866,208	10,936,394	59,193	16p13.13
NLRC5	16	56,989,557	57,083,520	93,964	16q13
IFNGR2	21	33,402,882	33,437,516	34,635	21q22.11

Table 3 – Genomic reference.

2.4 Digital cytometry

To investigate and quantify the immune cell composition in the TME of tumors having *CDK12* defects, we used the bulk tissue gene expression profiles (GEP) from RNA-seq data from both pPCa and mCRPC with the digital cytometry CIBERSORTx (CIBERSORTx) (39). This program uses bulk tissue GEP, compares the data with prior

knowledge of expression profiles from purified leukocytes, and estimates a tumor's relative immune abundance composition. We used the 'signature matrix' containing a validated leukocyte GEP of 22 human hematopoietic cell phenotypes, leukocyte gene signature matrix (LM22), to estimate the immune cell composition from the TME.

2.5 Computational and statistical analysis

We used a GNU/Linux environment to perform the quality control and quantify the raw reads to the human transcriptome. Subsequently, downstream analysis was performed in RStudio software (R Foundation for Statistical Computing, R v4.1.2). Pearson Correlation was used to analyze the normalized expression levels (coef. level = 0.95). A gene was considered differentially expressed when log2 foldchange > 1 was expressed from the reference group with a p-adjusted value (FDR) < 0.05. For the enrichment analysis, we used a cutoff value of 0.05.

3 Results

3.1 Clinical analysis

The material under study was obtained retrospectively from the cBioPortal public domain. The 58 cases, defined according to NCCN criteria, had the intermediate-risk disease (clinical stage T2b, or T2c, Gleason score of 7, or PSA = 10–20 ng/ml) and high-risk disease (clinical stage T3a or higher, Gleason score 8–10, or PSA >20 ng/ml). We divided our cases into two cohorts, primary and metastatic tumors. The pPCa cohort comprises 48 cases, approximately 63 years old (median), with clinical stages ranging from T2b to T4. Within these tumors, 62.5% were classified as MHC I high and 47.916% as MHC II high. The pPCa *CDK12*-defective MHC-I High exhibited a trend towards better overall survival compared to the MHC lower expression group ($p > 0.05$, Figure 3).

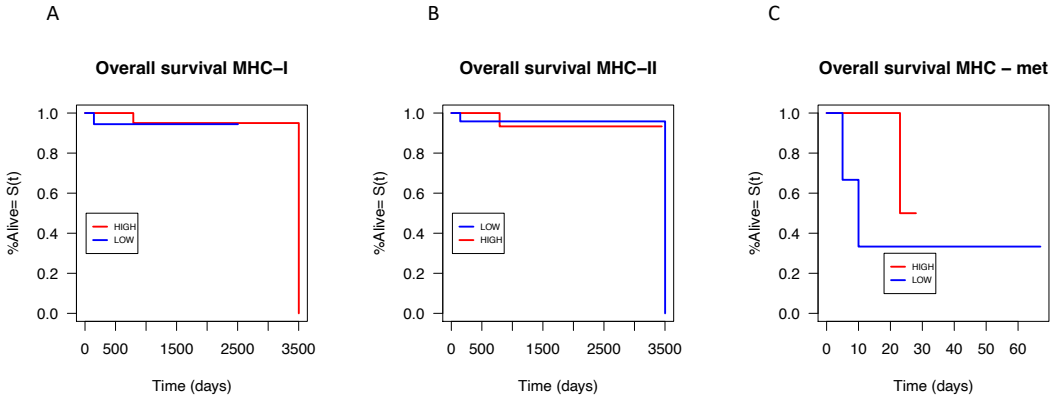

Figure 3 – Overall survival of *CDK12* defective patients

(A) Kaplan-Maier curve for overall survival in *CDK12* defective MHC-I High expressed primary tumors, (B) Kaplan-Maier curve for overall survival in *CDK12* defective MHC-II High expressed primary tumors and (C) Kaplan-Maier curve for overall survival in *CDK12* defective MHC High expressed metastatic tumors. Kaplan-Maier curve for overall survival was calculated using the *survfit* function from the survival package for R. The difference was not significant in all the comparisons ($p = 0.6$, $p = 1$, and $p = 0.5$, respectively). Log-rank statistic tests were performed using the *survdiff* function.

The mCRPC cohort comprises 10 cases, approximately 63 years old (median), with Gleason scores ranging from 6 to 9. Among them, 60% were classified as MHC High. The metastatic sites were bone, liver, lymph nodes, and soft tissues, and 50% of the tumors were treated with taxanes and 40% with Abiraterone plus enzalutamide. Tumors with higher MHC expression exhibited apparently better overall survival when compared to the MHC lower expression group ($p > 0.5$, Figure 3).

3.2 Transcriptomics alterations

Our working hypothesis for this study is that variation in the expression of the MHC genes among *CDK12* defective tumors could provide predictive information on poor ICB responses in this molecular subtype of prostate cancer. To investigate MHC expression levels in PCa further, we compared the transcriptomics of prostate tumors, including *CDK12* defective prostate tumors, classified as "MHC High" (top 75% quartile) to the transcriptomics of tumors classified as having a low expression of MHC genes (bottom 25% quartile).

3.2.1 *CDK12* defective MHC-I/-II High-expression tumors showed distinct transcriptome profiles with upregulation of IFN-γ-responsive genes and an inflamed TME

We first compared the transcriptome of *CDK12* defective tumors classified as MHC-High and MHC-Low (Figure 2). The 48 primary PCa *CDK12* defective MHC-I High showed 1319 upregulated and 2153 downregulated genes and showed four apparent clusters (Figure 4a). The upper cluster (I) has *IGHV* and *IGLV* over-expressed genes linked to *CDK12* MHC I high. The central clusters (II, III) have four HLA genes overexpressed in the MHC I high group, which supports our classification based on *CDK12* defective MHC expression (e.g., *HLA-A, HLA-B, HLA-C*). Also, this cluster showed an upregulation of many genes related to antigen presentation and CD8+ T cell activity. The lower cluster (IV) has 14 downregulated genes when MHC I is highly expressed. Likewise, *CDK12* defective MHC-II High exhibited 1129 upregulated and 580 downregulated genes. Our comparison showed two clusters (Figure 4b). The upper cluster showed the upregulation of genes related to cytotoxicity, immune cell migration, and immune suppression.

Analysis of the ten mCRPC tumors identified 230 upregulated and 46 downregulated genes that were differentially expressed in *CDK12* defective MHC-high and showed two distinct clusters (Figure 4c). The lower cluster showed the upregulation of genes linked to innate and adaptive immune response CD4+ and CD8+ T cell activity. In conclusion, for both primary PCa and metastatic CRPC, *CDK12* defective PCa that express higher MHC levels was associated with transcriptomic changes that indicate a general pattern of activation of IFN-γ-responsive and cytotoxic activity genes.

To better understand the transcriptional alterations in *CDK12* defective tumors classified as MHC-I/-II high-expressed, we used ORA and GSEA analysis to identify potential functional associations of expression changes associated with differentially expressed genes. In primary PCa, tumors with *CDK12* defective MHC-I and MHC-II high-expressed showed significant enrichment of pathways related to activation of immune cells and antigen presentation by MHC-I and MHC-II, as expected (Figure 4d). Furthermore, GSEA

results showed activation of many Hallmark's pathways in *CDK12* defective MHC-I high-expressed (e.g., Epithelial-Mesenchymal Transition, Inflammatory Response, Interferon Gamma Response, Interferon Alpha Response, TNFA Signaling via NFKB, P53, and IL2/STAT5 Signaling (Figure 5a). In addition, the *CDK12* defective MHC-II High group had similar pathway activation but with the addition of Allograft Rejection (Figure 5b).

The *CDK12* defective metastatic group with MHC high-expressed showed enrichment of cytotoxicity and adaptive cytotoxicity immune response (Figure 4f). In addition, GSEA results showed activation of various Hallmarks and Reactome pathways (e.g., Allograft Rejection, Interferon Gamma Response, Inflammatory Response, Interferon Alpha Response, IL2/STAT5 Signaling, Apoptosis, TCR Signaling, Interleukin 10 Signaling, Constitutive Signaling by Aberrant PI3K in Cancer, and the suppressive PD1 Signaling pathway) (Figure 5c-d). Our transcriptomic analysis suggests that CDK12 defective PCa expressing high MHC genes display the activation of various pathways associated with an active and inflamed tumor microenvironment.

3.2.2 *CDK12* defective MHC-I/-II High groups exhibited tumor microenvironment with high expression of chemokines and immunomodulatory genes.

We investigate the difference between chemokines and immunomodulatory gene expression to elucidate the underlying immunologic signature in TME of *CDK12* defective tumors expressing high MHC genes. In primary PCa, the *CDK12* defective MHC-I High exhibited upregulation of many chemokines linked to APCs and effector T cell migration and the immunomodulatory genes *HAVCR2* (*TIM3*) and *IDO1* (Figure 6a-b). Also, the MHC-II high group presented increased expression of chemokines related to Natural killer, T effector cell, and B cell infiltration, and the immuno-modulatory genes *CD274* (*PD-L1*), *HAVCR2* (*TIM3*), and *IDO1* (Figure 6c-e). Based on Pearson Correlation analysis, we observed a significant positive correlation between MHC-I complex genes and *IDO1* but with no other investigated gene. Interestingly, among the MHC-II genes, correlation analysis showed a significant positive association between the expression of the MHC-II complex and the immuno-modulatory genes *CD274* (*PD-L1*), *IDO1*, and *HAVCR2* (*TIM3*) (Figure 7a-b).

The *CDK12* defective metastatic group with high expression of MHC showed high expression of chemokines and the immunomodulatory gene *CD274* (*PD-L1*) (Figure 6f). Furthermore, we observed a significant positive association between the immunomodulatory genes *HAVCR2* (*TIM3*) and *CTLA4*, *LAG3*, and MHC-I and -II genes (Figure 7c-d). *CDK12* defective tumors' expression of higher levels of MHC genes shows a pattern of upregulation of chemokine and immunomodulatory mechanisms.

3.3 Tumor Microenvironment.

3.3.1 *CDK12* defective MHC-I/-II High CDK12 defective tumors showed distinct immune cell infiltrate in the TME.

Our transcriptomics analysis predicted that *CDK12* defective tumors expressing high levels of MHC-I/-II genes would display enrichment of immune cells with high effector and cytotoxic activity and the co-inhibitory expression of inhibitory pathways by tumor cells. We used in silico cytometry (CIBERSORTx) to test this hypothesis and to estimate the immune cell composition in the TME of *CDK12* defective tumors expressing high levels of MHC-I/-II genes.

In primary PCa, *CDK12* defective MHC-I high-expressed showed a significant increase in the composition of Naïve B cells, CD8+ T cells, and γδ T cells. In contrast, the reduced composition of Mastocytes (Figure 8a). In comparison, the MHC-II high-expressed group exhibited an increase of γδ T cells and reduced composition of Plasma cells and M0 macrophages (Figure 8b).

Additionally, the *CDK12* defective metastatic group with high expression of MHC showed a significative increased composition of CD8+ T cell and M1 Macrophages (Figure 8c). Our results generally indicate that *CDK12* defective PCa expressing higher levels of MHC displayed increased APCs and effector lymphocytes traffic in their TME.

3.4 Genomic Alterations

3.4.1 Genomics alterations of MHC-I/-II region associated with defective *CDK12*.

During tumor evolution, the infiltration of cytotoxic lymphocytes eliminates highly immunogenic tumor clones, causing a preferential selection and survival of cell populations that have acquired MHC alterations. To determine whether the low levels of MHC-I/-II genes in *CDK12* defective tumors were derived from somatic genomic alterations affecting antigen presentation genes, we used an allele-specific copy number algorithm to estimate the copy number profile of *CDK12* defective tumors expressing low levels of MHC-I/-II genes. The algorithm incorporates quantitative analysis of RNA-seq data derived from MHC-I/-II and HLA genes on chromosome 6 and several other genes, such as *PTEN*, commonly subject to LOH in PCa (40). Estimates include the determination of the relative clonality of allele-specific copy number alterations based on the fraction of tumor cells bearing LOH.

WES of primary PCa revealed both subclonal allele-specific copy-neutral losses of heterozygosity (CN-LOH) and complete loss of heterozygosity (LOH) events affecting

MHC-I/-II and HLA genes on chromosome 6. Both major clonal and minor subclonal events were detected by comparing the copy number to the estimated cellular fraction of tumor cells harboring the copy number alteration (Table 4 and Figure 9). One example is illustrated by tumor TCGA-KK-A8IA in which only one major clonal event was detected with a cellular fraction = 0.833, and LOH events were detected on chromosomes 2, 5, and 10. While TCGA-YL-A8HO revealed four subclonal events, capturing biallelic loss, CN-LOH, and LOH in chromosomes 2, 5, 6, 15, and 16. Tumors expressing lower levels of MHC-I/II genes may be associated with the somatic genomic LOH events affecting regional transcriptional regulators of MHC expression and the cis-acting regulatory components of the MHC (Table 4). Two patients also showed subclonal complete loss of the *B2M* locus (ID: TCGA-EJ-8471, cellular fraction = 0.37; TCGA-YL-A8HO, cellular fraction = 0.27. Table 4). Interestingly, *B2M* is an important component of the MHC-I complex, and mutations of this gene have previously been associated with ICB resistance (41).

In contrast to primary PCa, metastatic tumors harboring *CDK12* mutation expressing low levels of MHC-I/II showed allele-specific copy number gains in the MHC-I/II complex and key regulators of MHC expression (Table 5 and Figure 10). Interestingly, one patient showed a clonal LOH event at the *JAK2* and *B2M* loci (ID: 5115615, cellular fraction = 0.90).

These data indicate that low expression of MHC in primary tumor clones appears to be associated with frequent somatic CN-LOH and LOH subclonal genomic alterations in primary tumors harboring *CDK12* mutation. While metastatic tumors revealed both LOH and high copy-number gains affecting antigen presentation genes and their regulators. Therefore, these subclonal CN-LOH and LOH events are associated with impaired MHC expression that may contribute to reducing tumor immunogenicity.

Table 4 – *CDK12* defective in primary MHC low expressed tumors.

Patient ID	Gene	chrom	start	end	cellular fraction	Total copy number	Minor copy number
KK.A8IA	*STAT1*	2	134713128	192194260	0.833	1	0
KK.A8IA	*IRF1*	5	55231421	143147410	0.833	1	0
KK.A8IA	*PTEN*	10	87552401	89139399	0.833	1	0
KK.A8IA	*B2M*	15	41191425	77615398	0.208	0	0
KK.A8IG	*IFNGR1*	6	65302925	170584366	0.668	1	0
KK.A8I6	*PTEN*	10	73243437	104454566	0.332	0	0
KK.A8I6	*NLRC5*	16	49396608	90096324	0.11	0	0
XJ.A9DX	*NLRC5*	16	49280867	57722991	0.62	1	0
ZG.A9LM	*STAT1*	2	134317491	192057773	0.47	2	0

Continued...

Patient ID	Gene	chrom	start	end	cellular fraction	Total copy number	Minor copy number
ZG.A9LM	*B2M*	15	19882284	101922415	0.47	2	0
ZG.A9LM	*NLRC5*	16	56276055	89228602	0.47	2	0
EJ.8472	*JAK1*	1	21619903	67705610	0.37	1	0
EJ.8472	*B2M*	15	42751857	97971259	0.37	2	0
XQ.A8TA	*IRF2*	4	177976002	189984351	0.92	1	0
XQ.A8TA	*IRF1*	5	128464930		0.92	2	0
XQ.A8TA	*PTEN*	10	87790275	89599433	0.92	0	0
YL.A8HO	*STAT1*	2	119157673	199659594	0.12	0	0
YL.A8HO	*IRF1*	5	143082	181260211	0.38	2	0
YL.A8HO	MHC-I/II, *TAP1/2*	6	304637	170584276	0.27	1	0
YL.A8HO	*IFNGR1*	6	304637	170584276	0.27	1	0
YL.A8HO	*B2M*	15	19882294	101922415	0.27	1	0
YL.A8HO	*CIITA*	16	8644541	58196892	0.22	2	0
YL.A8HO	*NLRC5*	16	8644541	58196892	0.22	2	0
XK.AAJA	*PTEN*	10	7243639	12235132	0.54	1	0
KK.A7AP	*B2M*	15	33311111	57091863	0.87	1	0
KK.A7AP	*NLRC5*	16	48347484	90177833	0.87	1	0
HC.7744	*B2M*	15	42515191	45178103	0.12	0	0
KK.A8IG	*IFNGR1*	6	65302925	170584366	0.668	1	0
S EJ.7784	*JAK2*	9	14859	18718116	0.437	1	0
HC.A48F	*JAK1*	1	41513578	80451865	0.86	1	0
HC.A48F	*IRF2*	4	85671	189984257	0.21	1	0
HC.A48F	*IRF1*	5	54400082	171456817	0.86	1	0
HC.A48F	MHC-I/II, *TAP1/2*	6	304637	170584366	0.31	1	0
HC.A48F	*IFNGR1*	6	304637	170584366	0.31	1	0
HC.A48F	*PTEN*	10	49168049	118015066	0.21	1	0
HC.A48F	*B2M*	15	44380814	50749712	0.86	1	0
HC.A48F	*NLRC5*	16	35085998	90177833	0.86	1	0

[1]

[1] Integral results of FACETS analysis of whole-exome sequencing data from *CDK12* defective primary tumors expressing low levels of MHC-I/II. The table shows the integer copy number for the allelic ratio of the heterozygous SNPs in the tumor/normal pair for each patient. The first column is the patient ID and the second column is the MHC region loci and other genes commonly subject to LOH in PCa. The last two columns represent the total copy number and the minor copy number, respectively. Tumors

Table 5 – *CDK12* defective in metastatic MHC low expressed tumors.

ID	Gene	chrom	start	end	cellular fraction	Total copy number	Minor copy number
5115412	*JAK1*	1	33804897	68440771	0.49	5	2
5115412	*STAT1*	2	187346385	205615949	0.54	5	2
5115412	*IRF2*	4	182891198	185757023	0.87	6	2
5115412	*IRF1*	5	112892242	139881181	0.81	4	2
5115412	MHC-I	6	29555893	32256053	0.87	4	1
5115412	MHC-II	6	32288409	38345160	0.30	6	2
5115412	*TAP-1*	6	32288409	38345160	0.30	6	2
5115412	*TAP-2*	6	32288409	38345160	0.30	6	2
5115412	*JAK2*	9	2804198	15486990	0.59	4	2
5115412	*PTEN*	10	80253502	93958843	0.30	6	2
5115412	*B2M*	15	30626570	59138344	0.59	4	2
5115412	*CIITA*	16	198972	17358048	0.59	4	2
5115412	*NLRC5*	16	57372390	71634040	0.52	4	2
5115412	*IFGRR2*	21	33230307	34889712	0.87	5	2
1115161	*IRF2*	4	184116877	186709443	0.51	6	3
1115161	*HLA-A*	6	29330997	30628358	0.79	3	1
1115161	*HLA-B*	6	30635016	31382266	0.59	5	2
1115161	*HLA-C*	6	30635016	31382266	0.59	5	2
1115161	*JAK2*	9	52538	33113788	0.20	3	1
5115615	*JAK1*	1	63571201	65432064	0.912	3	1
5115615	*STAT1*	2	188522965	192194738	0.912	3	1
5115615	MHC-I	6	29944749	30415099	0.899	3	1
5115615	MHC-I/II	6	30469283	32407241	0.902	4	2
5115615	MHC-II	6	32439760	32666486	0.912	3	1
5115615	MHC-II/TAP1/2	6	32666737	34289022	0.902	4	2
5115615	*JAK2*	9	117666	9091026	0.906	1	0
5115615	*B2M*	15	41691484	46828068	0.906	1	0
5115615	*CIITA*	16	9938304	11178578	0.912	3	1
5115615	*IFGRR2*	21	33335636	37018290	0.899	3	1

Integral results of FACETS analysis of whole-exome sequencing data from CDK12 defective metastatic tumors expressing low levels of MHC-I/II. The same parameters shown in Table 1 were used to characterize LOH for each gene of interest. Metastatic PCa showed allele-specific copy number gains at *JAK1, STAT1, IRF2, IRF1, MHC-I/II, TAP1, TAP2, IFNR1, JAK2, B2M, CIITA, NLRC5*, and *IFNR1*. One patient showed a clonal LOH event at the *JAK2* and *B2M* loci (Total copy number/minor copy number ratio=1:0). *MHC-I = *HLA-A, HLA-B, and HLA-C; MHC-II = HLA-DRA, HLA-DRB5, HLA-DRB6, HLA-DPA1, HLA-DPB1, HLA-DQA1, HLA-DQB1*, and *HLA-DQB2*.

with a 2:1 ratio are considered normal for each position, while 2:0 and 1:0 represent CN-LOH and LOH events. The cellular fraction represents the estimated number of cells harboring the genotype. Primary PCa revealed subclonal CN-LOH and LOH at *JAK1, STAT1, IRF2, IRF1*, MHC-I/II, *TAP1, TAP2, IFNR1, JAK2, B2M, CIITA, NLRC5*, and *IFNR1*. Two patients showed biallelic loss at the *B2M* locus (Total copy number/minor copy number ratio=0:0). *MHC-I = *HLA-A, HLA-B, and HLA-C; MHC-II = HLA-DRA, HLA-DRB5, HLA-DRB6, HLA-DPA1, HLA-DPB1, HLA-DQA1, HLA-DQB1*, and *HLA-DQB2*.

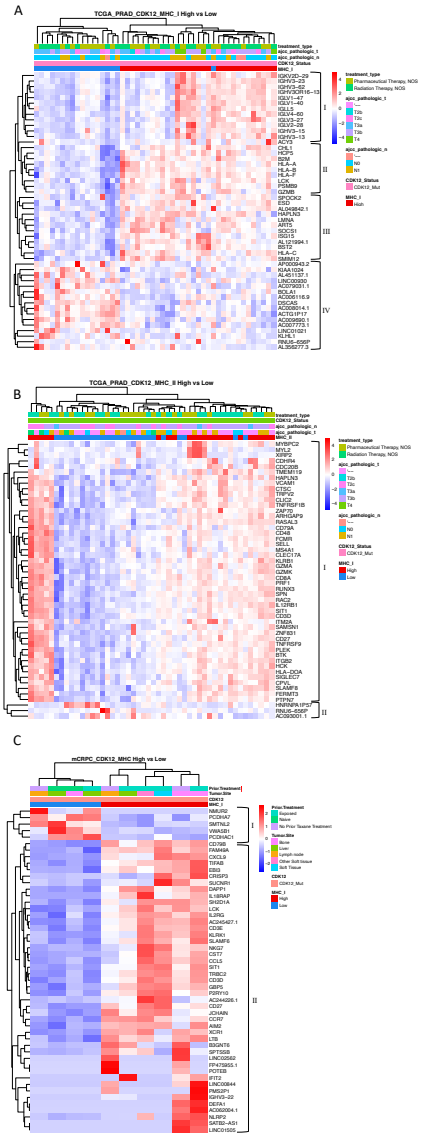

D

ID	Description	p.adjust
GO:0051249	regulation of lymphocyte activation	1,48E-19
GO:0002460	adaptive immune response based on somatic recombination of immune receptors built from immunoglobulin superfamily domains	1,48E-19
GO:0050867	positive regulation of cell activation	2,78E-20
GO:0002449	lymphocyte mediated immunity	1,16E-18
GO:0006958	complement activation, classical pathway	2,77E-14
GO:0006959	humoral immune response	1,08E-09
GO:0050853	B cell receptor signaling pathway	2,20E-08
GO:0002440	production of molecular mediator of immune response	7,15E-08
GO:0042742	defense response to bacterium	1,39E-07
GO:0006910	phagocytosis, recognition	5,66E-08

E

ID	Description	p.adjust
GO:0051249	regulation of lymphocyte activation	2,00E-25
GO:0042110	T cell activation	5,84E-25
GO:0050867	positive regulation of cell activation	9,60E-23
GO:0007159	leukocyte cell-cell adhesion	2,50E-20
GO:0002460	adaptive immune response based on somatic recombination of immune receptors built from immunoglobulin superfamily domains	2,80E-20
GO:0002443	leukocyte mediated immunity	3,53E-19
GO:1903037	regulation of leukocyte cell-cell adhesion	8,17E-19
GO:0070661	leukocyte proliferation	1,75E-15
GO:0046651	lymphocyte proliferation	5,77E-14
GO:0070663	regulation of leukocyte proliferation	1,64E-12

F

ID	Description	p.adjust
GO:0051251	positive regulation of lymphocyte activation	4,87E-15
GO:0002449	lymphocyte mediated immunity	6,43E-15
GO:0002253	activation of immune response	6,67E-15
GO:0042110	T cell activation	3,27E-11
GO:0002460	adaptive immune response based on somatic recombination of immune receptors built from immunoglobulin superfamily domains	1,76E-09
GO:0006959	humoral immune response	1,21E-06
GO:0019724	B cell mediated immunity	2,55E-06
GO:0050863	regulation of T cell activation	9,19E-07
GO:0007159	leukocyte cell-cell adhesion	3,27E-04
GO:1903037	regulation of leukocyte cell-cell adhesion	1,75E-03

Figure 4 – MHC-I/-II high expression in *CDK12* defective prostate cancer showed distinct transcriptome activity

(a) Transcriptome heatmap exhibiting clustering of top 50 DEGs in pPCa *CDK12*-Mut MHC-I High group (n = 30). The upper cluster (I) has IGHV and IGLV over-expressed genes linked to CDK12 MHC I high. The central clusters (II and III) has four HLA genes overexpressed in the MHC I high group, supporting our *CDK12* mutated MHC expression classification. The lower cluster (IV) has 14 downregulated genes when MHC I is highly expressed. (b) Transcriptome heatmap exhibiting clustering of top 50 DEGs in the pPCa *CDK12*-Mut MHC-II High group (n = 23). The upper cluster (I) has upregulating genes related to cytotoxicity, immune cell migration, and immune suppression. We could not observe clinical features associated with MHC I or II clusters. (c) Transcriptome heatmap exhibiting clustering of top 50 DEGs in the mCRPC *CDK12*-Mut MHC High group (n = 6). The combined MHC I and II showed two distinct clusters. The lower cluster showed the upregulation of genes linked to innate and adaptive immune response and CD4+ and CD8+ T cell activity. (d) Enriched GO (BP) pathways of the upregulated genes from pPCa *CDK12*-Mut MHC-I. (e) Enriched GO (BP) pathways of the upregulated genes from pPCa *CDK12*-Mut MHC-II High group. (f) Enriched GO (BP) pathways of the upregulated genes from the mCRPC *CDK12*-Mut High group. The DEGs are relative to the *CDK12*-Mut 'Low' group. Clinical information is displayed on top of the heatmap for each patient. The color scale in the heatmap represents the Z-score of the normalized read counts for each gene, where the red scale indicates upregulated and blue low-expressed genes. Enrichment analyses were performed using clusterProfiler and p-adjusted value = 0.05 as the cutoff. Bar plots show the top 20 most significant Gene Ontology (BP) terms.

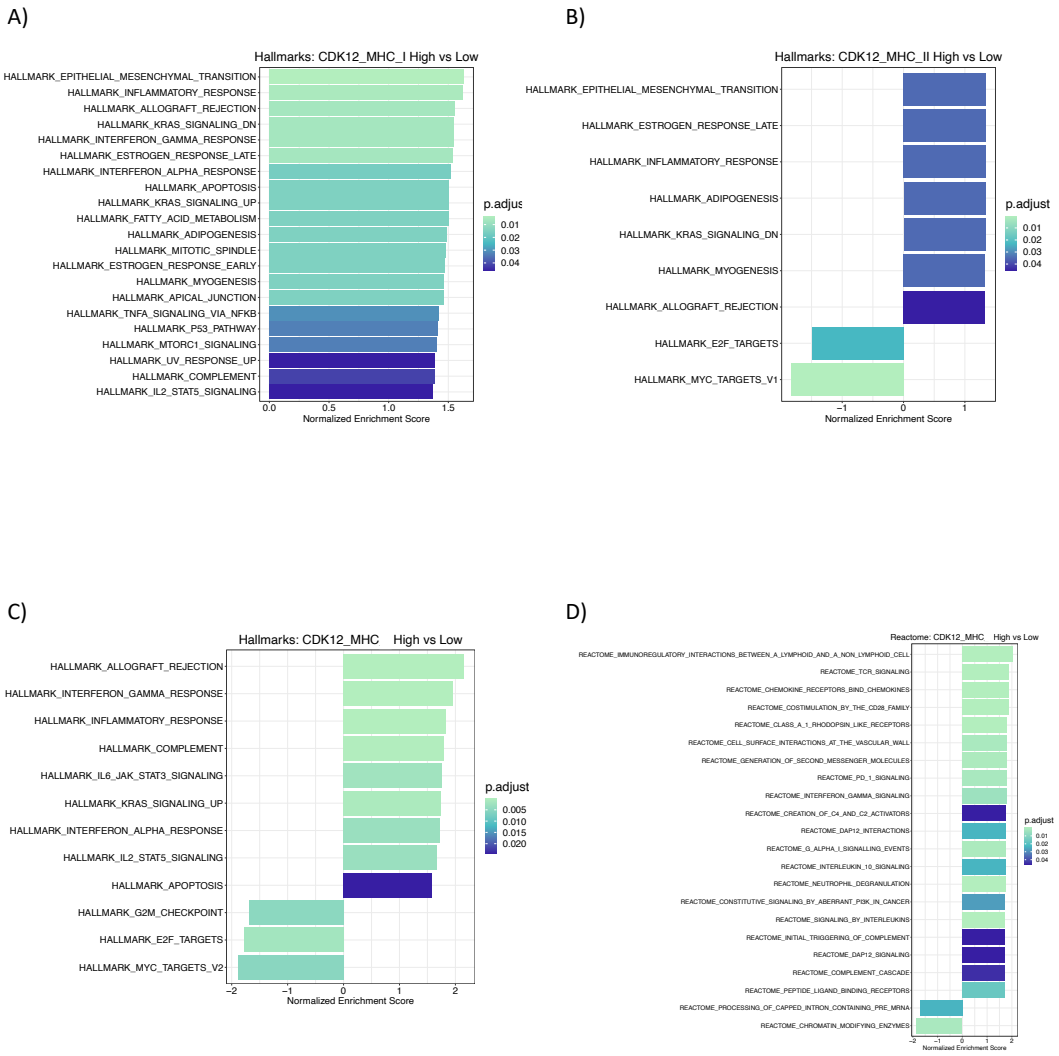

Figure 5 – MHC high expressed *CDK12* defective prostate tumors are associated with activation of immune-related pathways.

Gene Set Enrichment Analysis of Hallmark's pathways in pPCa *CDK12*-Mut MHC-I High (n = 30). (b) Gene Set Enrichment Analysis of Hallmark pathways in pPCa *CDK12*-Mut MHC-II High (n = 23). (c-d) Gene Set Enrichment Analysis of Hallmarks and Reactome pathways in mCRPC *CDK12*-Mut MHC High (n = 10). A normalized enrichment score indicates each factor's positive or negative association with the condition of interest, which means activation or suppression of the pathway. Enrichment analyses were performed using cluster-Profiler and p-adjusted value = 0.05 as the cutoff.

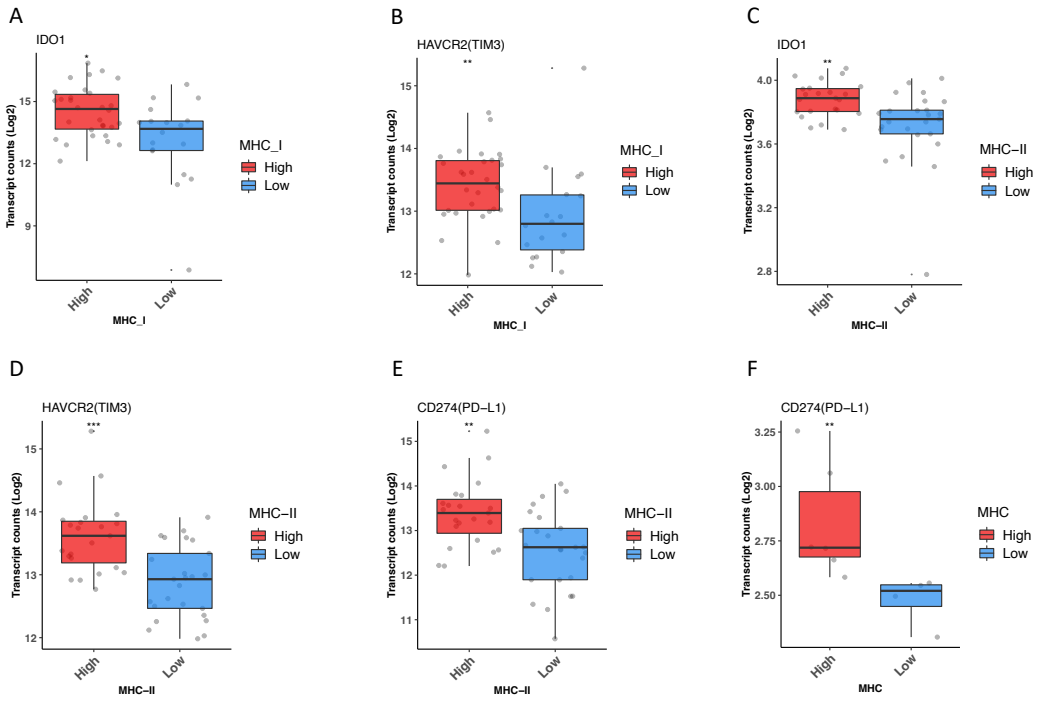

Figure 6 – MHC high expressed *CDK12* defective prostate cancer showed enhanced expression of immunomodulatory genes.

RNA-sequencing expression level of immunomodulatory genes (a) *IDO1* ($p < 0.018$), (b) *HAVCR2* (*TIM3*) ($p < 0.0022$) in *CDK12*-Mut MHC-I High. n = 48; (c) *CD274* (*PD-L1*) ($p < 0.0028$), (d) *HAVCR2* (*TIM3*) ($p < 0.00012$), (e) *IDO1* ($p < 0.001$) in *CDK12*-Mut MHC-II High. n = 48; (f) *CD274* (*PD-L1*) ($p < 0.0095$). n = 10; *: p-value < 0.05; **: p-value < 0.01, by Mann-Whitney test. *IDO1*, Indoleamine 2,3-Dioxygenase 1; *HAVCR3* (*TIM3*), T-Cell Immunoglobulin Mucin Receptor 3; *CD274* (*PD-L1*), Programmed Cell Death 1 Ligand 1.

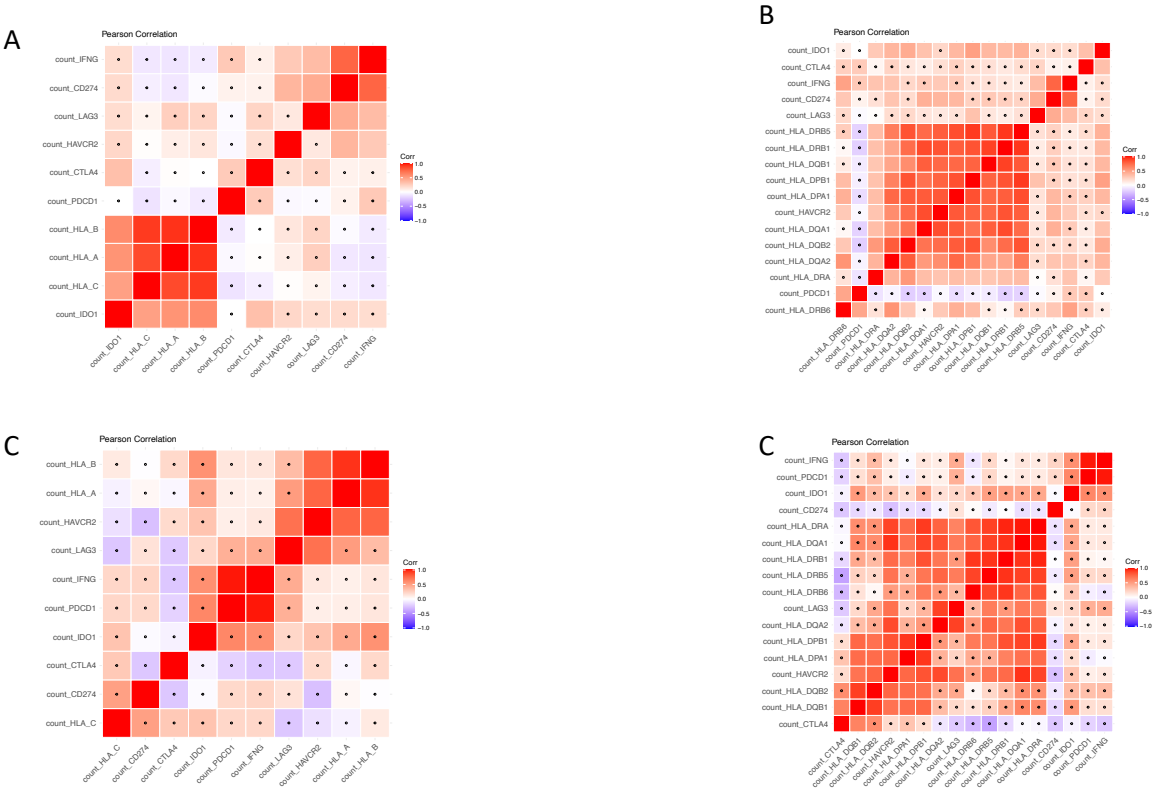

Figure 7 – Correlation of classical MHC and immunomodulatory genes.

(a-b) Correlation plots between MHC-I /–II and the immunomodulatory genes in primary prostate tumors. (c-d) Correlation plots between MHC-I /–II and the immunomodulatory genes in metastatic castration-resistant prostate tumors. Pearson Correlation was used in normalized expression levels of each gene (coef. level = 0.95). A significant correlation is indicated in nonmarket squares ($p<0.05$).

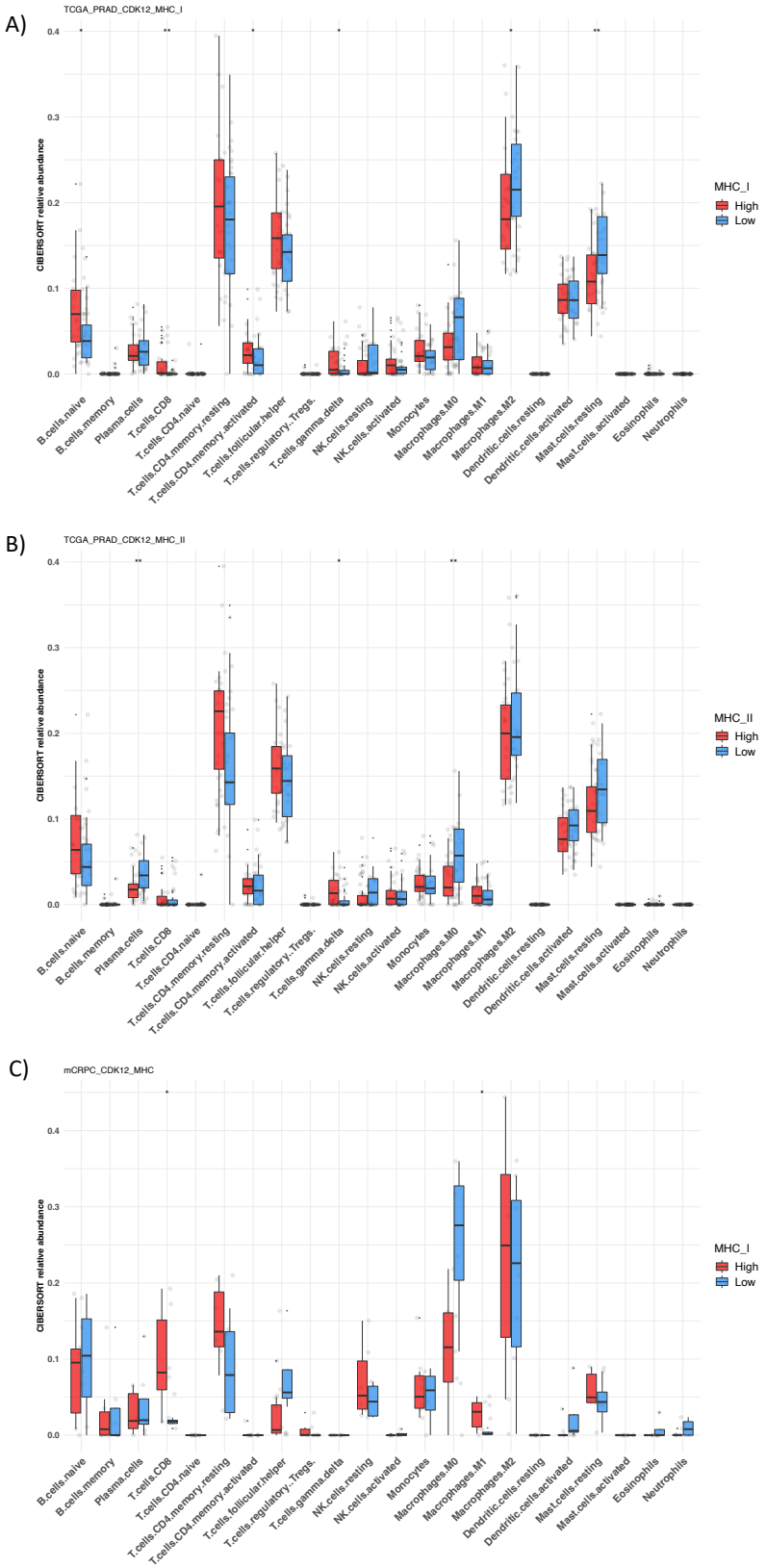

Figure 8 – MHC high expressed *CDK12* defective is associated with enhanced T cell recruitment of prostate tumors.

(a) CIBERSORT-derived immune cell abundance of 22 distinct cell subsets based on *CDK12* defective MHC-I High pPCa (n = 30). (b) CIBERSORT-derived immune cell abundance of 22 distinct cell subsets based on *CDK12* defective MHC-II High pPCa (n = 23). (c) CIBERSORT-derived immune cell abundance of 22 distinct cell subsets based on *CDK12* defective MHC High mCRPC (n = 10). *: p-value < 0.05; **: p-value < 0.01, by Mann-Whitney test.

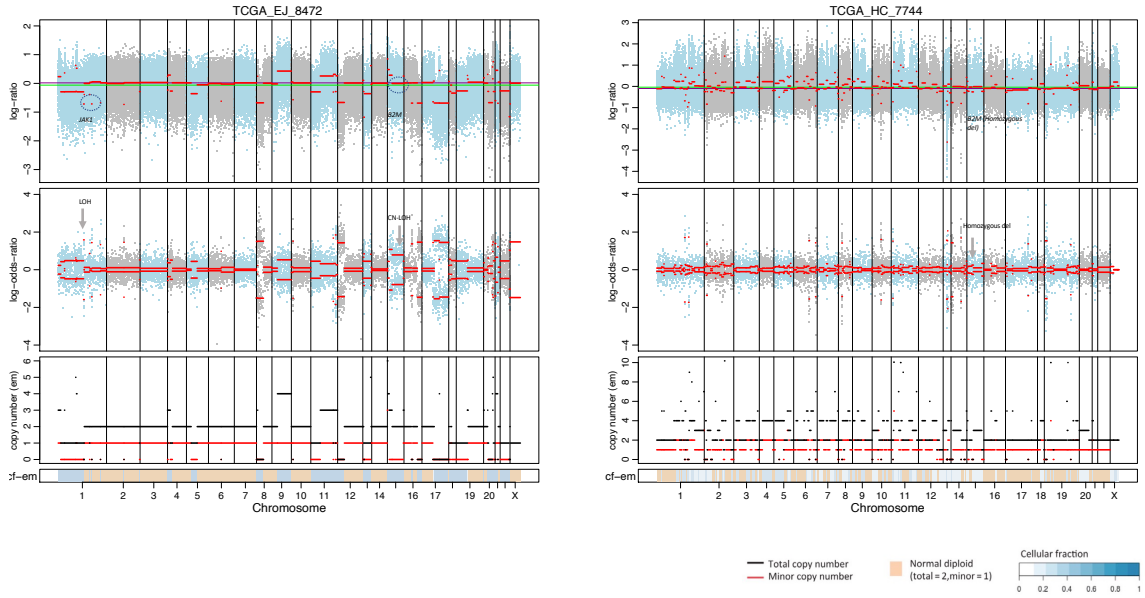

Figure 9 – Whole-genome sequencing data from *CDK12* defective in primary MHC low-expressed tumors.

Integrated visualization shows the total copy number log ratio (logR) on the top panel and allele-specific log-odds-ratio data (logOR) on the second panel with chromosomes alternating in blue and gray. The third panel plots the corresponding integer (total, minor) copy number calls. Tumors with a 2:1 ratio are considered normal for each position, while 2:0 and 1:0 represent CN-LOH and LOH events. The estimated cellular fraction profile is plotted at the bottom, revealing both clonal and subclonal copy number events.

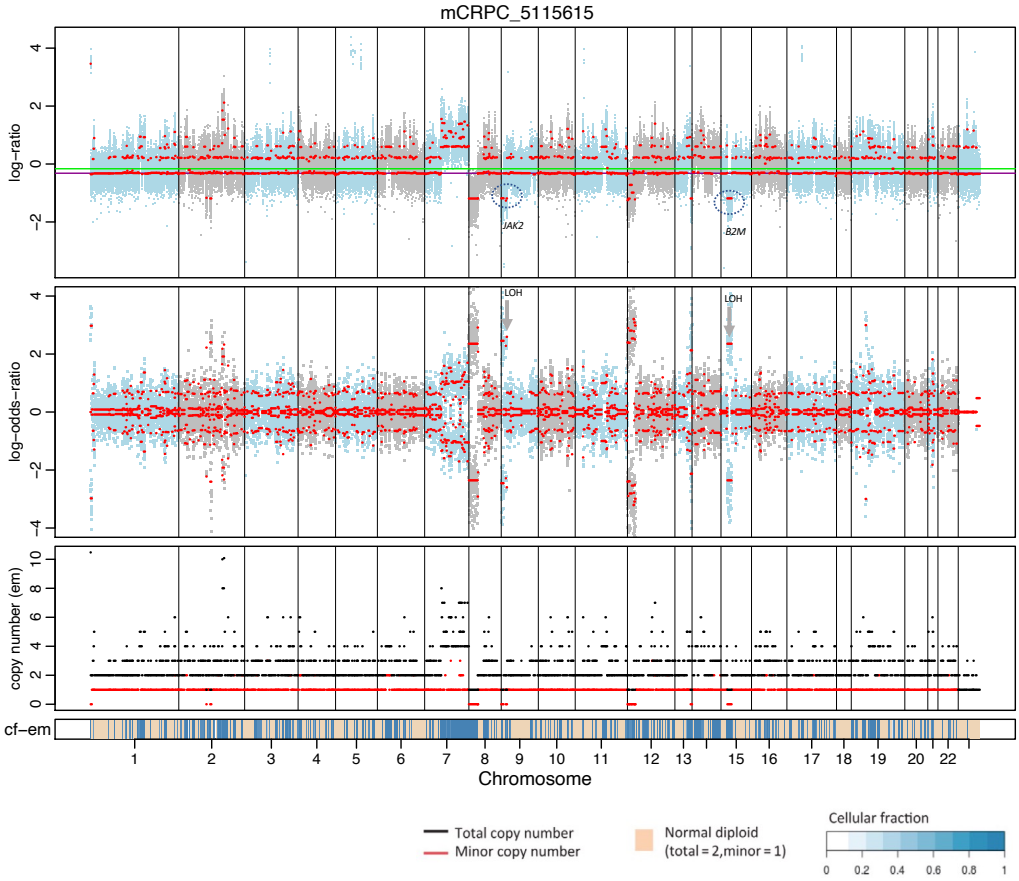

Figure 10 – Whole-genome sequencing data from *CDK12* defective in metastatic MHC low-expressed tumors.

Integrated visualization shows the total copy number log ratio (logR) on the top panel and allele-specific log-odds-ratio data (logOR) on the second panel with chromosomes alternating in blue and gray. The third panel plots the corresponding integer (total, minor) copy number calls. Tumors with a 2:1 ratio are considered normal for each position, while 2:0 and 1:0 represent CN-LOH and LOH events. The estimated cellular fraction profile is plotted at the bottom, revealing both clonal and subclonal copy number events.

4 Discussion

In prostate cancer, *CDK12* inactivation is known to increase the immunogenicity of tumor cells (42, 43, 7, 44, 45). Changes in MHC-I and -II expression are involved in tumor immune evasion in various types of cancer (46, 47, 37, 34). Using RNA-seq data, we observed two groups of *CDK12* defective tumors regarding MHC expression. Tumors expressing higher levels of MHC showed the activation of multiple pathways associated with the immune system, significantly high expression of immunomodulatory genes, and increased CD8+ T cells, B cells, γδ T cells, and M1 Macrophages composition in their TME. Also, Tumors with low MHC expression showed allele-specific copy-number alteration in genes involved in regulating MHC expression and antigen presentation.

Analysis of the clinical data showed that higher expression of MHC genes in pPCa and mCRPC, respectively, exhibited a trend towards better overall survival when compared to the MHC lower expression group ($p > 0.05$, Figure 3). Several studies have found similar expression relationships of the MHC-I and -II genes associated with better clinical outcomes and different resistance mechanisms (48, 20, 49). Lack of MHC-I expression in melanoma was linked to higher odds of progressive disease and resistance to anti-CTLA4 but not anti-PD1 (20). In the same study, expression of MHC-II in tumors was associated with tumors more likely to respond to anti-PD1 treatment. MHC-II expression was linked to a positive outcome in Hodgkin Lymphoma treated with nivolumab (anti-PD1) (49). Park et al. showed that MHC-II positivity in tumor cells was associated with better disease-free survival in patients with lymph node metastasis (48). From a practical standpoint, these results suggest that analysis of MHC-I and -II expression levels would be developed to determine whether *CDK12* defective prostate tumors expressing higher levels of MHC genes are more likely to respond to ICB treatments.

Transcriptomic signatures associated with MHC expression variation have been described in different tumor types (34). These signatures capture the activity of genes and biological pathways related to tumor cells' cross-talk with the TME and appear to correlate with clinical responses to ICB (50, 51, 20, 34). Ayers et al. proposed a gene expression profile with eighteen genes relevant to predicting the clinical outcome of anti-PD1 therapy (52). This IFN-γ gene signature in pre-treatment tumor biopsies was associated with better results in melanoma, head-and-neck squamous cell carcinoma, and gastric cancer treated with pembrolizumab. In our study, the *CDK12* patient tumors expressing high levels of MHC genes showed upregulation of the IFN-γ gene signature, which might reflect a better response to anti-PD1 therapy (Figure 11). Our results also showed pathways' activation related to IFN-γ response in the pPCA and mCRPC cohorts (Figure 4b-f and Figure 5b-d.

An IFN-γ gene signature can alternatively activate the expression of immunomodulatory mechanisms and promote adaptive resistance to therapeutic anti-PD1 (53, 54). IFN-γ is a central actor in the elimination phase during immunoediting (55). However, exacerbated levels of IFN-γ are also associated with developing protumor molecular mechanisms leading to an immuno-

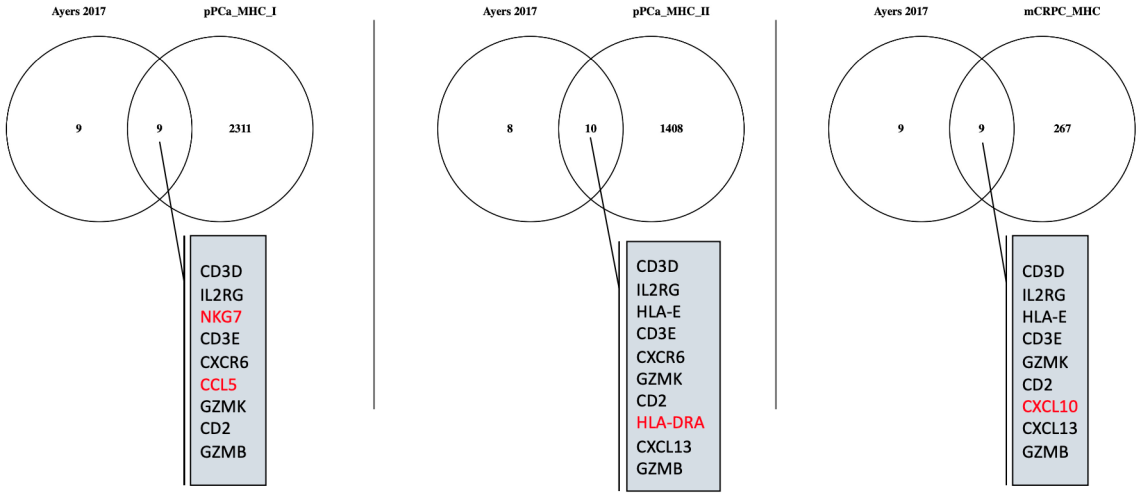

Figure 11 – Common activation of IFN-γ-responsive genes in *CDK12* defective MHC high expressed tumors.

In our study, the *CDK12* patient tumors classified as MHC High showed the presence of several genes previously described as IFN-γ-responsive and cytotoxic activity and associated with response to anti-PD1 therapy (52). Common genes with Ayers et al. 2017, are indicated in the intersection and unique features for each comparison are indicated in red. Venn's Diagrams by Oliveros, J.C. (2007-2015) Venny. An interactive tool for comparing lists with Venn's diagrams. *https://bioinfogp.cnb.csic.es/tools/venny/index.html.*

suppressive and tolerogenic TME (53). We identified the upregulation of immunomodulatory molecules, such as *IDO1, TIM3*, and *CD274(PD-L1)*, in both prostate tumors expressing higher levels of MHC-I and -II genes (Figure 6). Interestingly, the *CDK12* patient tumors expressing high levels of MHC genes showed the presence IFN-γ gene signature, including upregulation of a non-classical MHC molecule (*HLA-E*), which is known regulator of NK cell and CTL (56, 57). We also found a link between *IGHV* and *IGLV* over-expressed genes in a group of the *CDK12* defective pPCa expressing high levels of MHC-I (Figure 4a, upper cluster I). The production of Ig by tumor cells (cancer-derived Ig) is described in various tumors and prostate cancer (58, 59, 60, 61). Also, cancer-derived Ig may act as checkpoint proteins and inhibit effector T cells and NK cells (58, 62). Our findings indicate the presence of an acquired resistance mechanism in a subset of *CDK12* defective prostate tumors expressing high levels of MHC genes. We suppose that measuring the basal expression of MHC genes would be developed as a biomarker to characterize *CDK12* patient samples with a previously inflamed environment and which would reflect the expression of immunomodulatory genes linked to resistance to anti-PD1.

The expression of MHC molecules plays a pivotal role in providing the signals necessary to recognize and activate the immune system against tumor neoantigens and is essential to controlling tumor growth through cytotoxic activity (63, 55). We found a higher abundance of CD8+ T cells in *CDK12* defective tumors expressing high levels of MHC genes (Figure 8). This result may either indicate the dependence of CD8+ T cells in MHC-I antigen presentation or suggest that enhanced CD4+ Th infiltrate could support the continued accumulation of CD8+ CTLs in the tumor microenvironment (50). Interestingly, *CDK12* pPCa with high expression of both MHC-I and -II genes showed increased levels of γδ T cells (Figure 8a-b). The basal effector

immune cell population, such as γδ T cells in pPCa, may contribute to IFN-γ signaling and indicate the dependence of the MHC-unrestricted recognition role of γδ T cells and its presence in the TME (64, 20).

The loss of MHC expression derived from two different disruption means (65). First, regulatory abnormalities downregulate the expression of MHC genes through mechanisms that do not affect the genomic structure of HLA genes. Specific T-cells can recover the MHC expression-mediated response (e.g., IFN-γ signaling) in such cases. Second, during tumor evolution, the infiltration of cytotoxic lymphocytes eliminates tumor clones highly immunogenic, causing a selection of clones that may present structural alteration, or "Hard" lesions, in the MHC loci or other genomic regions (e.g., *B2M, IFN, STAT*) distinct from the derived clone (41).

Genomic studies of chromosome 6 in various cancers suggest reduced MHC expression is often associated with genetic and LOH aberrations that may result in reduced antigen presentation and, thus, facilitate immune evasion (16, 66). In keeping with these data, our WES of pPCa and mCRPC revealed CN-LOH and LOH in *CDK12* defective tumors expressing low levels of MHC-I/II genes at known regulators of MHC expression and the components of the MHC (Tables 4 5). Two pPCa patients also showed complete loss of the *B2M* locus, while one mCRPC exhibited a LOH event at the *B2M*, an important component of the MHC-I complex (41). These results indicate that after selection, the low expression of MHC genes is derived from tumor clones harboring "Hard" genomics alterations comprising loci involved in normal MHC expression. Therefore, these clones will be invisible to the immune system and contribute to tumor progression.

This study has a number of limitations. First, future studies in many patients harboring *CDK12* mutations are needed to address potential statistical bias regarding our low number of patients. Second, we did not address the potential molecular mechanism underlying the alteration of the low expression of MHC in *CDK12* defective prostate cancer, including epigenetic alterations and miRNA activity. Further studies are needed to approach the causes of MHC disruption derived from "Soft" alterations that occur in *CDK12* defective prostate cancer. Third, because the non-tumor cell content was not defined in this study, we could not establish a limit for the contribution of the *CDK12* defective tumor cells and TME to the MHC expression since the RNA-seq relies on data from bulk tissue.

5 Conclusion

We distinguished two sets of *CDK12* defective tumors based on differential MHC expression levels. Our data suggest that *CDK12* defective PCa expressing higher levels of classical MHC genes have an active and inflamed tumor microenvironment with elevated immunomodulatory pathway expression and increased presence of effector T cells. Tumors with decreased MHC expression showed copy-number alteration in genes that regulate MHC expression and antigen presentation. More extensive *in vitro* and *in vivo* investigations are required to relate this molecular subtype to potential actionable immunomodulatory mechanisms or possible therapeutic targets in PCa. These findings also support investigations into the clinical use of MHC expression levels in *CDK12* defective prostate cancer to identify tumors likely to respond to ICB treatment.

Bibliography

1 REBELLO, R. J. et al. Prostate cancer. *Nature Reviews Disease Primers*, Nature Research, v. 7, 12 2021. ISSN 2056676X.

2 WONG, M. C. et al. Global incidence and mortality for prostate cancer: Analysis of temporal patterns and trends in 36 countries. *European Urology*, v. 70, p. 862–874, 11 2016. ISSN 03022838.

3 BINNEWIES, M. et al. Understanding the tumor immune microenvironment (time) for effective therapy. *Nature Medicine*, Nature Publishing Group, v. 24, p. 541–550, 5 2018. ISSN 1546170X.

4 MELO, C. et al. The role of somatic mutations on the immune response of the tumor microenvironment in prostate cancer. *International Journal of Molecular Sciences*, v. 22, 2021. ISSN 14220067.

5 SCHUMACHER, T. N.; SCHREIBER, R. D. Neoantigens in cancer immunotherapy. *Science*, American Association for the Advancement of Science, v. 348, p. 69–74, 4 2015. ISSN 10959203.

6 WU, Y. M. et al. Inactivation of cdk12 delineates a distinct immunogenic class of advanced prostate cancer. *Cell*, Cell Press, v. 173, p. 1770–1782.e14, 6 2018. ISSN 10974172.

7 SOKOL, E. S. et al. Pan-cancer analysis of cdk12 loss-of-function alterations and their association with the focal tandem-duplicator phenotype. *The Oncologist*, Oxford University Press (OUP), v. 24, p. 1526–1533, 12 2019. ISSN 1083-7159.

8 NGUYEN, L. et al. Pan-cancer landscape of homologous recombination deficiency. *Nature Communications*, Nature Research, v. 11, 12 2020. ISSN 20411723.

9 RESCIGNO, P. et al. Characterizing cdk12-mutated prostate cancers a c. *Clinical Cancer Research*, American Association for Cancer Research Inc., v. 27, p. 566–574, 1 2021. ISSN 15573265.

10 ANTONARAKIS, E. S. et al. Cdk12 -altered prostate cancer: Clinical features and therapeutic outcomes to standard systemic therapies, poly (adp-ribose) polymerase inhibitors, and pd-1 inhibitors. *JCO Precision Oncology*, American Society of Clinical Oncology (ASCO), p. 370–381, 11 2020. ISSN 2473-4284.

11 SPRANGER, S.; GAJEWSKI, T. F. Mechanisms of tumor cell-intrinsic immune evasion. *Annu. Rev. Cancer Biol*, v. 2, p. 213–228, 2018. Disponível em: <https://doi.org/10.1146/annurev-cancerbio->.

12 LI, X. et al. Wnt/β-catenin signaling pathway regulating t cell-inflammation in the tumor microenvironment. *Frontiers in Immunology*, Frontiers Media S.A., v. 10, 9 2019. ISSN 16643224.

13 HORTON, B. L.; FESSENDEN, T. B.; SPRANGER, S. Tissue site and the cancer immunity cycle. *Trends in Cancer*, Cell Press, v. 5, p. 593–603, 10 2019. ISSN 24058033.

14 MCGRANAHAN, N. et al. Allele-specific hla loss and immune escape in lung cancer evolution. *Cell*, Cell Press, v. 171, p. 1259–1271.e11, 11 2017. ISSN 10974172.

15 THIBODEAU, J.; BOURGEOIS-DAIGNEAULT, M.-C.; LAPOINTE, R. Targeting the mhc class ii antigen presentation pathway in cancer immunotherapy. *OncoImmunology*, v. 1, p. 908–916, 9 2012. ISSN 2162-402X.

16 DHATCHINAMOORTHY, K.; COLBERT, J. D.; ROCK, K. L. Cancer immune evasion through loss of mhc class i antigen presentation. *Frontiers in Immunology*, Frontiers Media S.A., v. 12, 3 2021. ISSN 16643224.

17 GARRIDO, F.; APTSIAURI, N. Cancer immune escape: Mhc expression in primary tumours versus metastases. *Immunology*, Blackwell Publishing Ltd, v. 158, p. 255–266, 12 2019. ISSN 13652567.

18 ALGARRA, I.; GARRIDO, F.; GARCIA-LORA, A. M. Mhc heterogeneity and response of metastases to immunotherapy. *Cancer and Metastasis Reviews*, Springer, v. 40, p. 501–517, 6 2021. ISSN 15737233.

19 WATSON, N. F. et al. Immunosurveillance is active in colorectal cancer as downregulation but not complete loss of mhc class i expression correlates with a poor prognosis. *International Journal of Cancer*, v. 118, p. 6–10, 1 2006. ISSN 00207136.

20 RODIG, S. J. et al. Mhc proteins confer differential sensitivity to ctla-4 and pd-1 blockade in untreated metastatic melanoma. *Sci. Transl. Med*, v. 10, p. 3342, 2018. Disponível em: <https://www.science.org>.

21 GAO, J. et al. Integrative analysis of complex cancer genomics and clinical profiles using the cbioportal. *Science Signaling*, v. 6, 4 2013. ISSN 19450877.

22 ABESHOUSE, A. et al. The molecular taxonomy of primary prostate cancer. *Cell*, Cell Press, v. 163, p. 1011–1025, 11 2015. ISSN 10974172.

23 IMADA, E. L. et al. Recounting the fantom cage associated transcriptome. *bioRxiv*, 2019. ISSN 2692-8205.

24 PATRO, R. et al. Salmon provides fast and bias-aware quantification of transcript expression. *Nature Methods*, Nature Publishing Group, v. 14, p. 417–419, 2017. ISSN 15487105.

25 LOVE, M. I.; HUBER, W.; ANDERS, S. Moderated estimation of fold change and dispersion for rna-seq data with deseq2. *Genome Biology*, BioMed Central Ltd., v. 15, 12 2014. ISSN 1474760X.

26 ZHU, A.; IBRAHIM, J. G.; LOVE, M. I. Heavy-tailed prior distributions for sequence count data: Removing the noise and preserving large differences. *Bioinformatics*, Oxford University Press, v. 35, p. 2084–2092, 6 2019. ISSN 14602059.

27 SUBRAMANIAN, A. et al. *Gene set enrichment analysis: A knowledge-based approach for interpreting genome-wide expression profiles*. 2005. Disponível em: <www.pnas.orgcgidoi10.1073pnas.0506580102>.

28 KHATRI, P.; SIROTA, M.; BUTTE, A. J. Ten years of pathway analysis: Current approaches and outstanding challenges. *PLoS Computational Biology*, v. 8, 2 2012. ISSN 1553734X.

29 LIBERZON, A. et al. The molecular signatures database hallmark gene set collection. *Cell Systems*, Cell Press, v. 1, p. 417–425, 12 2015. ISSN 24054712.

30 SONESON, C.; LOVE, M. I.; ROBINSON, M. D. Differential analyses for rna-seq: transcript-level estimates improve gene-level inferences. *F1000Research*, v. 4, p. 1521, 12 2015. ISSN 2046-1402.

31 CARBON, S. et al. The gene ontology resource: 20 years and still going strong. *Nucleic Acids Research*, Oxford University Press, v. 47, p. D330–D338, 1 2019. ISSN 13624962.

32 WU, T. et al. clusterprofiler 4.0: A universal enrichment tool for interpreting omics data. *The Innovation*, Cell Press, v. 2, 8 2021. ISSN 26666758.

33 KOOPMAN, L. A. et al. Multiple genetic alterations cause frequent and heterogeneous human histocompatibility leukocyte antigen class i loss in cervical cancer. *Journal of Experimental Medicine*, v. 191, p. 961–976, 3 2000. ISSN 0022-1007.

34 SCHAAFSMA, E. et al. Pan-cancer association of hla gene expression with cancer prognosis and immunotherapy efficacy. *British Journal of Cancer*, Springer Nature, v. 125, p. 422–432, 8 2021. ISSN 15321827.

35 SHEN, W. et al. Seqkit: A cross-platform and ultrafast toolkit for fasta/q file manipulation. *PLOS ONE*, v. 11, p. e0163962, 10 2016. ISSN 1932-6203.

36 BAILEY, M. H. et al. Comprehensive characterization of cancer driver genes and mutations. *Cell*, Cell Press, v. 173, p. 371–385.e18, 4 2018. ISSN 10974172.

37 MONTESION, M. et al. Somatic hla class i loss is a widespread mechanism of immune evasion which refines the use of tumor mutational burden as a biomarker of checkpoint inhibitor response. *Cancer Discovery*, v. 11, p. 282–292, 2 2021. ISSN 2159-8274.

38 SHEN, R.; SESHAN, V. E. Facets: allele-specific copy number and clonal heterogeneity analysis tool for high-throughput dna sequencing. *Nucleic Acids Research*, v. 44, p. e131–e131, 9 2016. ISSN 0305-1048.

39 NEWMAN, A. M. et al. Robust enumeration of cell subsets from tissue expression profiles. *Nature Methods*, Nature Publishing Group, v. 12, p. 453–457, 4 2015. ISSN 15487105.

40 JAMASPISHVILI, T. et al. Clinical implications of pten loss in prostate cancer. *Nature Reviews Urology*, v. 15, p. 222–234, 4 2018. ISSN 1759-4812.

41 ZARETSKY, J. M. et al. Mutations associated with acquired resistance to pd-1 blockade in melanoma. *New England Journal of Medicine*, Massachusetts Medical Society, v. 375, p. 819–829, 9 2016. ISSN 0028-4793.

42 JUAN, H. C. et al. Cdk12 is essential for embryonic development and the maintenance of genomic stability. *Cell Death and Differentiation*, Nature Publishing Group, v. 23, p. 1038–1048, 6 2016. ISSN 14765403.

43 DUBBURY, S. J.; BOUTZ, P. L.; SHARP, P. A. Cdk12 regulates dna repair genes by suppressing intronic polyadenylation. *Nature*, Nature Publishing Group, v. 564, p. 141–145, 12 2018. ISSN 14764687.

44 LI, Y. et al. Cdk12/13 inhibition induces immunogenic cell death and enhances anti-pd-1 anticancer activity in breast cancer. *Cancer Letters*, Elsevier Ireland Ltd, v. 495, p. 12–21, 12 2020. ISSN 18727980.

45 LOTAN, T. L.; ANTONARAKIS, E. S. Cdk12 deficiency and the immune microenvironment in prostate cancer. *Clinical Cancer Research*, American Association for Cancer Research Inc., v. 27, p. 380–382, 1 2021. ISSN 15573265.

46 GARRIDO, F.; RUIZ-CABELLO, F.; APTSIAURI, N. Rejection versus escape: the tumor mhc dilemma. *Cancer Immunology, Immunotherapy*, Springer Science and Business Media Deutschland GmbH, v. 66, p. 259–271, 2 2017. ISSN 14320851.

47 APTSIAURI, N. et al. Regressing and progressing metastatic lesions: Resistance to immunotherapy is predetermined by irreversible hla class i antigen alterations. In: . [S.l.: s.n.], 2008. v. 57, p. 1727–1733. ISSN 03407004.

48 PARK, I. A. et al. Expression of the mhc class ii in triple-negative breast cancer is associated with tumor-infiltrating lymphocytes and interferon signaling. *PLOS ONE*, v. 12, p. e0182786, 8 2017. ISSN 1932-6203.

49 ROEMER, M. G. M. et al. Journal of clinical oncology major histocompatibility complex class ii and programmed death ligand 1 expression predict outcome after programmed death 1 blockade in classic hodgkin lymphoma. 2018. Disponível em: <https://doi.org/10.1200/JCO.2017.>

50 JOHNSON, D. B. et al. Melanoma-specific mhc-ii expression represents a tumour-autonomous phenotype and predicts response to anti-pd-1/pd-l1 therapy. *Nature Communications*, Nature Publishing Group, v. 7, 1 2016. ISSN 20411723.

51 JOHNSON, D. B. et al. Quantitative spatial profiling of pd-1/pd-l1 interaction and hla-dr/ido-1 predicts improved outcomes of anti-pd-1 therapies in metastatic melanoma. *Clinical Cancer Research*, American Association for Cancer Research Inc., v. 24, p. 5250–5260, 11 2018. ISSN 15573265.

52 AYERS, M. et al. Ifn-γ-related mrna profile predicts clinical response to pd-1 blockade. *Journal of Clinical Investigation*, American Society for Clinical Investigation, v. 127, p. 2930–2940, 8 2017. ISSN 15588238.

53 ZAIDI, M. R.; MERLINO, G. The two faces of interferon-γ in cancer. *Clinical Cancer Research*, v. 17, p. 6118–6124, 10 2011. ISSN 1078-0432.

54 KOYAMA, S. et al. Adaptive resistance to therapeutic pd-1 blockade is associated with upregulation of alternative immune checkpoints. *Nature Communications*, Nature Publishing Group, v. 7, 2 2016. ISSN 20411723.

55 SCHREIBER, R. D.; OLD, L. J.; SMYTH, M. J. *Cancer Immunoediting: Integrating Immunity's Roles in Cancer Suppression and Promotion*. 2011. Disponível em: <www.sciencemag.org>.

56 BORST, J. et al. Cd4+ t cell help in cancer immunology and immunotherapy. *Nature Reviews Immunology*, Nature Publishing Group, v. 18, p. 635–647, 10 2018. ISSN 14741741.

57 SALOMé, B. et al. Nkg2a and hla-e define an alternative immune checkpoint axis in bladder cancer. *Cancer Cell*, v. 40, n. 9, p. 1027–1043.e9, 2022. ISSN 1535-6108. Disponível em: <https://www.sciencedirect.com/science/article/pii/S1535610822003695>.

58 LI, X. et al. The presence of ighg1 in human pancreatic carcinomas is associated with immune evasion mechanisms. *Pancreas*, v. 40, p. 753–761, 7 2011. ISSN 0885-3177.

59 PAN, B. et al. Suppression of ighg1 gene expression by sirna leads to growth inhibition and apoptosis induction in human prostate cancer cell. *Molecular Biology Reports*, v. 40, p. 27–33, 1 2013. ISSN 0301-4851.

60 QIN, C. et al. Cancer-driven igg promotes the development of prostate cancer though the sox2-cigg pathway. *The Prostate*, v. 80, p. 1134–1144, 9 2020. ISSN 0270-4137.

61 CUI, M. et al. Immunoglobulin expression in cancer cells and its critical roles in tumorigenesis. *Frontiers in Immunology*, v. 12, 3 2021. ISSN 1664-3224.

62 WANG, Z. et al. Cancer-derived sialylated igg promotes tumor immune escape by binding to siglecs on effector t cells. *Cellular Molecular Immunology*, v. 17, p. 1148–1162, 11 2020. ISSN 1672-7681.

63 QIN, H. et al. Specific antitumor immune response induced by a novel dna vaccine composed of multiple ctl and t helper cell epitopes of prostate cancer associated antigens. *Immunology Letters*, v. 99, p. 85–93, 6 2005. ISSN 01652478.

64 BORN, W. K.; REARDON, C. L.; O'BRIEN, R. L. The function of γδ t cells in innate immunity. *Current Opinion in Immunology*, v. 18, p. 31–38, 2 2006. ISSN 09527915.

65 GARRIDO, F.; CABRERA, T.; APTSIAURI, N. "hard" and "soft" lesions underlying the hla class i alterations in cancer cells: Implications for immunotherapy. *International Journal of Cancer*, v. 127, p. 249–256, 7 2010. ISSN 00207136.

66 GARRIDO, M. A. et al. Copy neutral loh affecting the entire chromosome 6 is a frequent mechanism of hla class i alterations in cancer. *Cancers*, MDPI, v. 13, 10 2021. ISSN 20726694.

67 LAUTERT-DUTRA, W. et al. Quantitative mhc class-i/-ii gene expression levels in cdk12 mutated prostate cancer reveal intratumorally t cell adaptive immune response in tumors. *bioRxiv*, Cold Spring Harbor Laboratory, 2022. Disponível em: <https://www.biorxiv.org/content/early/2022/12/21/2022.04.16.487364>.

Appendix

APPENDIX A – Supplementary Information

All programming scripts used to access, manage, and run QC, mapping, quantification, and normalization pipelines, and so forth can be found at our GitHub repository link: https://github.com/WilliamLautertD/RNA-Seq-Uro-Lab—FMRP-USP. The complete DEGs and Enriched pathways lists, together with the altered genomics regions for each patient are also publicly shareable and available on *Biorxiv* LAUTERT-DUTRA et al., 2022 (67) or upon request from the author.

APPENDIX B – Data access provided by Database of Genotype and Phenotype (dbGaP)(NIH)

Project Request

Project #29255 : Impact of CDK12 mutation on Immune Response in Prostate Cancer

Project name	Impact of CDK12 mutation on Immune Response in Prostate Cancer
Project ID	29255
Approved user name	JEREMY SQUIRE
Institute affiliation	UNIVERSITY OF SAO PAULO RIBEIRAO PRETO (Non-Profit)
Request date : 2022-06-23	Previous renewal date : 2022-06-23 Next Renewal date : 2023-06-01

Applicant Organization

Legal Name :	**UNIVERSITY OF SAO PAULO RIBEIRAO PRETO**						
Department :	Medicine			Division :			
Street 1 :	Avenida Bandeirantes						
City :	Ribeirão Preto	State :	São Paulo	Zip :		Country :	Brazil

PI Contact Information

Name :	**JEREMY SQUIRE**			Position :	Professor		
Organization:	UNIVERSITY OF SAO PAULO RIBEIRAO PRETO						
Street 1 :	Avenida Bandeirantes 3900						
City :	Ribeirão Preto	State :	SP	Zip :	14049-900	Country :	Brazil
Phone :	55 (16) 997874143	:		Email :	squirej@fmrp.usp.br		

SO Contact Information

Name :	**Fabiana Valera**			Position :	Signing Official		
Organization:	UNIVERSITY OF SAO PAULO RIBEIRAO PRETO						
Street 1 :	Av. Bandeirantes, 3900						
City :	Ribeirao Preto	State :	Sao Paulo	Zip :	14049-900	Country :	Brazil
Phone :	551636021000	:		Email :	facpvalera@fmrp.usp.br		

IT Director Contact Information

Name :	**Isabel Italiano**			Position :	Director		
Organization:	UNIVERSITY OF SAO PAULO RIBEIRAO PRETO						
Department :	CIRP/USP			Division :	UNIVERSITY OF SAO PAULO RIBEIRAO PRETO		
Street 1 :	Avenida Bandeirantes						
City :	Ribeirão Preto	State :	São Paulo	Zip :	14049900	Country :	Brazil
Phone :	551633153527	:		Email :	isabel.italiano@usp.br		

Project Request

Project #29255 : Impact of CDK12 mutation on Immune Response in Prostate Cancer

Approved Research Use Statement

Background: Treatment of advanced prostate cancer (PCa) remains a therapeutic challenge. Moreover, new immunotherapies like immune-checkpoint blockade (ICB) have shown significant benefits in only a minority of patients. CDK12 defect-PCa is a recently discovered molecular subtype of this tumor with a high neoantigen load and increased immune cell infiltrate. This molecular subtype is more common in mCRPC and the affected patients showed low overall survival and worse outcome. CDK12 defective PCa has variable results with recent immunotherapy clinical trials. The goal of this project is to identify the contribution of CDK12 somatic mutations to transcriptomic changes in tumors that increase the immune evasion capacity of prostate cancer (PCa). Methods: We will identify somatic mutations that affect CDK12 alleles in both primary and metastatic prostate cancer. Transcriptome analysis using RNA-Seq data of pPCa (PRAD-TCGA) and metastatic tumors from the dbGap database (phs000909.v1.p1, phs000915.v2.p2,phs000673.v4.p1) will be divided into CDK12-unmutated wild-type (CDK12 +/+, wt) and CDK12-mutated (CDK12+/-; CDK12-/-, mut) tumors. We will classify either heterozygous tumors with a mutation that will inactivate transcript on one allele (CDK12 +/-) and homozygous tumors with two mutations that will inactivate the gene on both alleles (CDK12 -/-). We will compare CDK12-wt vs. CDK12 +/-, CDK12-wt vs. CDK12 -/-, and CDK12 +/- vs. CDK12 -/- to investigate the biology of CDK12 loss of function and its relationship to the transcriptional profile and signaling pathways associated with antigen presentation and immune evasion. Digital cytometry will also be used to determine the relative abundances of any infiltrating immune cells of both CDK12-wt (CDK12 +/+) and CDK12-mutated tumors (CDK12 +/-; CDK12-/-, mut).). Implications: An improved understanding of the molecular basis of the CDK12-dependent immune evasion phenotype will provide additional information about the causes of immunotherapy failure in PCa. The Principal Investigator (Dr. Jeremy A. Squire) and the Signing Officer (Dr. Fabiana Cardoso Pereira Valera) are both full-time members of the University of Sao Paulo.

Non-Technical Summary

The results of immunotherapy in advanced prostate cancer (PCa) have been disappointing showing significant benefits in only a minority of patients. PCa with defects of the CDK12 gene have a distinctive mutational signature and increased immune cell infiltration. These alterations in tumors are usually predictive of good immunotherapy response, but clinical trials with CDK12 mutated PCa have had variable results. In this study, we will compare the global gene expression of a series of PCa CDK12 mutated tumors to PCa without these defects. This comparison will provide an understanding of gene expression differences characteristic of CDK12 mutated PCa and will be used to identify what molecular signals are associated with immunotherapy failure in PCa. Methods: We will identify tumor mutations that affect CDK12 alleles in both primary and metastatic prostate cancer. The results will be correlated with the changes in the global gene expression profile and the relative abundances of immune cells of both CDK12-normal vs. CDK12-mutated PCa using the dbGaP data. Implications: An improved understanding of the gene expression differences in CDK12-mutated PCa will provide crucial information about the molecular signaling in tumors leading to immunotherapy failure in PCa.

Collaborators

Internal

William Dutra
M.Sc. Candidate
UNIVERSITY OF SAO PAULO RIBEIRAO PRETO -- Department: Medicine -- Division: Genetics
Avenida Bandeirantes 3900
Ribeirão Preto, São Paulo 14049900 Brazil
Phone: +55 51 9 96633689 Email: williamlautert@usp.br

Change Log

Date	Changed Details
2022-06-23 13:00	Research Progress, Intellectual Property
2022-06-23 13:00	Publications and Manuscripts
2022-06-23 13:00	Presentations
2022-06-23 13:00	Intellectual Property
2022-06-23 13:00	Inappropriate Data Use
2021-09-22 13:00	Research Use Statement, Organization

Project Request

Project #29255 : Impact of CDK12 mutation on Immune Response in Prostate Cancer

2021-06-18 13:00	Collaborators
2021-05-28 12:00	Collaborators
2021-05-28 11:00	Research Use Statement, Public Summary

Project Request

Project #29255 : Impact of CDK12 mutation on Immune Response in Prostate Cancer

Consent Group(s) Information

phs000178.v11.p8 : The Cancer Genome Atlas (TCGA)

DUC : see attached

DAR : 104701

Request Date : 2021-06-21 Last Renewal Date : 2022-06-24

Name : General Research Use

Consent Group # : 1

Abbreviation : GRU

Data Use Limitation : Use of the data is limited only by the terms of the model Data Use Certification.

phs000673.v4.p1 : University of Michigan Clinical Sequencing Exploratory Research (CSER)

DUC : see attached

DAR : 107177

Request Date : 2021-09-24 Last Renewal Date : 2022-06-24

Name : General Research Use

Consent Group # : 1

Abbreviation : GRU

Data Use Limitation : Use of the data is limited only by the terms of the model Data Use Certification.

phs000915.v2.p2 : Integrative Clinical Sequencing Analysis of Metastatic Castration Resistant Prostate Cancer Reveals a High Frequency of Clinical Actionability

DUC : see attached

DAR : 103603

Request Date : 2021-06-08 Last Renewal Date : 2022-06-24

Name : Disease-Specific (Cancer, MDS)

Consent Group # : 2

Abbreviation : DS-CA-MDS

Data Use Limitation : Use of the data must be related to Cancer.
Use of the data includes methods development research (e.g., development of software or algorithms).

DAR : 103604

Request Date : 2021-06-11 Last Renewal Date : 2022-06-24

Name : Disease-Specific (Prostate Cancer, MDS)

Consent Group # : 1

Abbreviation : DS-PC-MDS

Data Use Limitation : Use of the data must be related to Prostate Cancer.
Use of the data includes methods development research (e.g., development of software or algorithms).

APPENDIX C – Scientific Activities

All working time was dedicated to journal clubs and lab meetings, literature reviews, classes, bioinformatic analysis, courses, scientific events attendance, and the production of scientific papers. This work led to ten presentations/published abstracts in congresses or meetings, one book chapter, and two publications. Additionally, four articles are in preparation, of which two as a leading author are under review (Annex A and B), and one invited editorial (Annex C). Worth mentioning, during this master's course, I attended an international training course in the bioinformatic field (Workshop on Genomics in Cesky Krumlov, Czech Republic).

Abstracts:

2021
66th Brazilian Congress of Genetics:

Lautert-Dutra, W.; Vidotto, T.; Melo, C.M.; Squire, J. A. Impact of *CDK12* loss on immune response in TCGA prostate tumors. In: Anais 66th Brazilian Congress of Genetics, 2021. Access: https://sbg.org.br/anais

Chaves, L. P.; Caliari, Andre L.; **Lautert-Dutra, W.**; Melo, C.M.; Picanço-de-Albuquerque, C.G.; Vidotto, T; Saggioro, F.P.; Reis, R.; Squire, J. A. Analysis of the relationships between *ZEB1*, *PTEN* loss, *TMPRSS2-ERG* fusion and immune response biomarkers in Prostate Cancer. 2021. 66th Brazilian Congress of Genetics, 2021. Access: https://sbg.org.br/anais.

Melo, C.M.; Vidotto, T; **Lautert-Dutra, W.**; Chaves, L. P.; Reis, R. B.; Squire, J.A. TCGA analysis identifies distinct genomic features of oncogenic progression and outcome associated with hemizygous *PTEN* loss tumors. 2021. In: Anais 66th Brazilian Congress of Genetics, 2021. Access: https://sbg.org.br/anais

2022
AACR – Annual Meeting:

Lautert-Dutra, W., Melo, C.M., Chaves, L.P., Caliari, A.L., Silva, F.C.S., Squire, J.A. Differential gene expression related to *TMPRSS2-ERG* fusion, *CDK12, RB1, TP53, AR* and *ZEB1* based on transcriptomic analysis of the TCGA-PRAD cohort.

Chaves, L.P., Caliari, A.L., **Lautert-Dutra, W.**, Silva, F.C.S., Melo, C.M., Saggioro, F.P., Reis, R.B., Squire, J.A. Analysis of the impact of *ZEB1* expression on pathway enrichment and immune cell abundance in prostate cancer.

VIII International Symposium on Translational Oncology (BARRETOS, SP):

Melo CM, Vidotto T, **Lautert-Dutra, W.**, Chaves LP, Reis RB, Squire JA. Pan-Cancer TCGA analysis identifies distinct genomic features of oncogenic progression and outcome associated with hemizygous *PTEN* loss tumors.

Chaves, L.P., Caliari, A.L., **Lautert-Dutra, W.**, Silva, F.C.S., Melo, C.M., Saggioro, F.P., Reis, R.B., Bayani, J; Squire, J.A. *SNAI1* expression is associated with clinically relevant pathways charges in Prostate Cancer.

67th Brazilian Congress of Genetics:

Lautert-Dutra, W., Melo, C.M., Chaves, L.P., Reis, R.B., Squire, J.A. Quantitative MHC class-I/II expression levels in *CDK12*-mutated prostate cancer patients reveal intratumorally T cell adaptative immune response in tumors.

Chaves, L.P., Caliari, A.L., **Lautert-Dutra, W.**, Silva, F.C.S., Melo, C.M., Saggioro, F.P., Reis, R.B., Squire, J.A. In silico analysis of epithelial-to-mesenchymal markers in prostate cancer identifies pathways associated with immune evasion activity.

Sousa e Silva, F.C.; **Lautert-Dutra, W.**,Melo, C.M., Squire, J.A. In-silico comparison of differentially expressed genes and immune evasion pathways in prostate cancer tumors with *PTEN, TP53*, and *TMPRSS2-ERG* alterations.

Book chapter:

Chaves, L.P., Melo, C.M., **Lautert-Dutra, W.**, Caliari, A.L., Squire, J.A. Transcriptomics and immune response in human cancer. *Transcriptomics in Health and Disease*, edited by G. A. Passos. Springer Nature. 2022.

Publications:

Melo, C.M.; Vidotto, T; Chaves, L. P.; **Lautert-Dutra, W.**; Reis, R. B.; Squire, J.A. The Role of Somatic Mutations on the Immune Response of the Tumor Microenvironment in Prostate Cancer. *Int. J. Mol. Sci.* 2021, 22, 9550. https://doi.org/10.3390/ijms22179550

Vidotto, T.; Melo, C.M.; **Lautert-Dutra, W.**; Chaves, L.P.; Reis, R.B.; Squire, J.A. Pan-cancer genomic analysis shows hemizygous *PTEN* loss tumors are associated with immune evasion and poor outcome. *Scientific Reports*, 2023. https://doi.org/10.1038/s41598-023-31759-6

Papers in the submission process:

Quantitative MHC class-I/-II classical gene expression levels in *CDK12* mutated prostate cancer patients reveal intratumorally T cell adaptive immune response in tumors. **Lautert-Dutra, W.**; Melo, C.M.; Chaves, L.P.; Crozier, C.; Saggioro, F.P.; Reis, R.B.; Bayani, J. Bonatto, S.; Squire, J.A. Under review *BMC Medical Genomics* (2023). (*Biorxiv* LAUTERT-DUTRA et al., 2022).

Tumor-agnostic biomarkers are predictive of tumor progression and biochemical recurrence in prostate cancer. **Lautert-Dutra, W.**; Melo, C.M.; Chaves, L.P.; Souza e Silva; Crozier, C.; Sundby A.E. ; Woroszchuk E.; Saggioro, F.P.; Squire, J.A.; Bayani, J. Under review in *Laboratory Investigation.*

Expression of epithelial-mesenchymal transition markers *SNAI1* and *ZEB1* promotes transcriptional alterations to promote tumor progression and immune evasion in prostate cancer. Chaves, LP; Melo, CM; **Lautert-Dutra, W.**; Crozier, C.; Sundby A.E. ; Woroszchuk E.; Reis, RB; Bayani, J. Squire, J.A. In preparation for the *Journal of Biomedical Science*.

Reduced *TP53* expression is associated with immune signaling and the inflammatory tumor microenvironment in prostate cancer. Sousa e Silva, F.C.; Melo, C. M.; **Lautert-Dutra, W.**; Chaves, L; Crozier, C.; Sundby A.E. ; Woroszchuk E.; Reis, RB; Bayani, J. Squire, J.A. In preparation for the *Pathobiology*.

Invited Editorial:

Precision medicine for prostate cancer— improved outcome prediction for low-intermediate risk disease using a six gene copy number alteration classifier. **Lautert-Dutra, W**; Reis, R.B.; Squire, J.A. *British Journal of Cancer*, 2023. (BJC-EDFV3343756)

Courses and Workshops:

Workshop on Genomics, Cesky Krumlov, Czech Republic. https://evomics.org. 2022. 80h.

Immuno-Oncology, HMX Pro Immunology, Harvard University, USA. Certificate of achievement: https://hrvd.io/adf9a676. 2021

Cancer Genomics and Precision Oncology, HMX Pro Genetics, Harvard University, USA. Certificate of achievement: https://hrvd.io/b3ffdd62. 2021.

Extension Programs and teaching:

Instructor at the *Curso de Verão em Genética*, 2022. “BIOINFORMÁTICA: ANÁLISE DE TRANSCRIPTOMA COM DADOS DE RNA-SEQ”

Annex

ANNEX A – Lautert-Dutra, W. *et al.* 2023. Under review in *BMC Medical Genomics*

Quantitative MHC class-I/-II gene expression levels in CDK12 mutated prostate cancer reveal intratumorally T cell adaptive immune response in tumors.

Lautert-Dutra, W.[1]; Melo, C.M.[1]; Chaves, L.P.[1];
Crozier, C.[2]; Saggioro, F.P.[3]; Reis, R.B.[3,4];
Bayani, J.[2,5]; Bonatto, S.[6]; Squire, J.A[1,7].

[1] Department of Genetics, Medical School of Ribeirao Preto, University of São Paulo, Ribeirao Preto 14048-900, SP, Brazil.

[2] Diagnostic Development, Ontario Institute for Cancer Research, Toronto, ON, Canada. [3] Department of Pathology, Ribeirão Preto Medical School, University of Sao Paulo, Ribeirão Preto, SP, Brazil

[4] Division of Urology, Department of Surgery and Anatomy, Medical School of Ribeirao Preto, University of São Paulo, Ribeirao Preto 14048-900, SP, Brazil.

[5] Laboratory Medicine and Pathobiology, University of Toronto, Toronto, ON, Canada.

[6] School of Health and Life Sciences, Pontifical Catholic University of Rio Grande do Sul, Av. Ipiranga, 668, 90619-900, Porto Alegre, RS, Brazil

[7] Department of Pathology and Molecular Medicine, Queen's University, Kingston, ON K7L3N6, Canada.

ANNEX B – Lautert-Dutra, W. *et al.* 2023. Under review in *Laboratory Investigation*

Tumor-agnostic biomarkers are predictive of tumor progression and biochemical recurrence in prostate cancer.

William Lautert-Dutra[1], Camila M. Melo[1], Luiz P. Chaves[1], Francisco C. Souza e Silva[2], Cheryl Crozier[6], Adam E. Sundby[6], Elizabeth Woroszchuk[6], Fabiano P. Saggioro[3], Felipe S. Avante[2], Rodolfo B. dos Reis[2], Jeremy A. Squire[1,4], Jane Bayani*[,5,6]

[1] Department of Genetics, Medical School of Ribeirao Preto, University of São Paulo, Ribeirao Preto 14048-900, SP, Brazil.

[2] Division of Urology, Department of Surgery and Anatomy, Medical School of Ribeirao Preto, University of São Paulo, Ribeirao Preto 14048-900, SP, Brazil.

[3] Department of Pathology, Ribeirão Preto Medical School, University of Sao Paulo, Ribeirão Preto, SP, Brazil

[4] Department of Pathology and Molecular Medicine, Queen's University, Kingston, ON K7L3N6, Canada.

[5] Laboratory Medicine and Pathobiology, University of Toronto, Toronto, ON, Canada.

[6] Diagnostic Development, Ontario Institute for Cancer Research, Toronto, ON, Canada.

ANNEX C – Lautert-Dutra, W. *et al.* 2023. Editorial for the *British Journal of Cancer* on the impact of a new six-gene copy number assay to distinguish between low- and intermediate-risk PCa

Precision medicine for prostate cancer— improved outcome prediction for low-intermediate risk disease using a six gene copy number alteration classifier.

William Lautert-Dutra[1], Rodolfo B. dos Reis[2], Jeremy A. Squire[1,3]

[1] Department of Genetics, Medical School of Ribeirão Preto, University of São Paulo, Ribeirão Preto 14048-900, SP, Brazil.

[2] Division of Urology, Department of Surgery and Anatomy, Medical School of Ribeirão Preto, University of São Paulo, Ribeirão Preto 14048-900, SP, Brazil.

[3] Department of Pathology and Molecular Medicine, Queen's University, Kingston, ON K7L3N6, Canada.

[4] Laboratory Medicine and Pathobiology, University of Toronto, Toronto, ON, Canada.